Chapter 7
Improvement of Gelation of Peanut Protein Isolate

Peanut protein isolate (PPI) has a variety of functional characteristics such as emulsibility, water-binding capacity, gelation, solubility, foamability, and film-forming property, so it can be used in meat products, aquatic products, baked food, dairy products, beverages, ice cream, candy, and other food treatment areas. Among them, as one of the major functional characteristics of PPI, gelation can make the protein have high viscosity, plasticity, and springiness, so that the gel formed by protein can be used as the carrier for water, flavor agents, sugar, and other compounds. Over the years, the study in this field has been the focus of food treatment research, and a majority of scholars have attached much attention to it. In order to further improve the gelation of PPI and expand its applications in the field of food treatment, modification method is often used for improvement. Physical modification (microwave, ultrahigh pressure, and other technologies) is simple, safe, and fast with low treatment costs, and it is able to maintain the nutritional value of protein to the largest extent, so it has gained popularity from the majority of scholars. There are a large number of study reports on the physical modification of peanut protein, but the study progress is slow due to the complexity of the globular structure of peanut protein. Although the functional characteristics of peanut protein can be improved in different degrees, the specific physical modification for gelation and its mechanism and other problems have not been described clearly, and thus the use of gelation of peanut protein has not been really industrialized. Therefore, it is urgent to deeply study the new technology, new methods, and related basic theories of the physical modification of peanut protein. High-pressure technology has been widely used in the modification studies of food protein (Messens et al. 1997; Wang et al. 2008; Apichartsrangkoon 2003; Molina et al. 2001, 2002; Puppo et al. 2004, 2005; Hongkang Zhang et al. 2003). Studies showed that the emulsibility, solubility, gelation, and other functional characteristics of soy protein, soy protein components, whey protein, and other protein might change due to high pressure. There are few studies on the ultrahigh-pressure modification of the functional characteristics of peanut protein, and the change laws of functional characteristics after modification and its structure-function

Q. Wang, *Peanut Processing Characteristics and Quality Evaluation*,
DOI 10.1007/978-981-10-6175-2_7

relationship are not clear, and there is no ultrahigh-pressure modification technology suitable for deep treatment. Therefore, the author's study team took the ultrahigh-pressure technology as the supporting point to modify the PPI and reveal the change law of its gelation and its structure-function relationship, so as to provide theoretical guidance to the deep treatment and utilization of peanut protein.

1 Ultrahigh-Pressure Modification

In the meat industry, especially in the production of ham, in order to reduce the cost while maintaining the sensory and nutritional quality of ham, a certain amount of soy protein can be added, which mainly makes use of the gelation, water-binding capacity, oil-binding capacity, and other functional characteristics of soy protein. Compared with soy protein, peanut protein has more advantages: firstly, peanut protein is a kind of plant protein with high nutritional value, so its nutritional value is similar to that of animal protein, and it does not contain cholesterol; secondly, peanut protein contains a large number of essential amino acids that can be absorbed by human bodies easily and has a seductive fragrance and white color. However, there is still a certain gap in the gelation, water-binding capacity, oil-binding capacity, and other functional characteristics between natural peanut protein and soybean protein, so the applications of natural peanut protein in meat products are limited. As we all know, ultrahigh-pressure technology is a physical process, the non-covalent bond of food ingredients will be destroyed or formed, and the enzymes, proteins, and other biological macromolecules will lose their activity and have denaturation, and the color, flavor, and taste deterioration of food and nutrient loss and other disadvantages caused by traditional hot treatment after the high-pressure treatment of food materials will be avoided (Murchie et al. 2005). There are also reports on increasing the solubility and emulsification of PPI by ultrahigh-pressure modification (Zong Wei and Chen Yi-ping 2007, 2008). In order to obtain high-gelatinized PPI, the author's team studied the change law of gelation of PPI under different ultrahigh-pressure treatment conditions, and the optimal ultrahigh-pressure treatment technology was obtained by response surface design on this basis, so as to provide a certain theoretical basis for the applications of PPI in the applications of ham and sausage.

Add deionized water to peanut protein powder at the ratio of 1:10, adjust the PH value to be 9.0 using 0.2 M NaOH solution, stir it for 2 h for extraction at room temperature (25 °C), and then centrifuge it for 10 min at 4200 r/min; adjust the PH value of supernate to about 4.5, centrifuge it again, remove the supernate, stir it evenly after adding a small amount of water, and then freeze and dry it for use. The protein content of sample was $86.46 \pm 0.09\%$ (protein conversion factor was 5.46), ash was $3.35 \pm 0.25\%$, water content was $4.12 \pm 0.13\%$, crude fat content was $0.60 \pm 0.08\%$, and total sugar content was $5.47 \pm 0.10\%$.

1.1 Single-Factor Test

The high-pressure treatment method has been improved on the basis of the report of Cong-Gui Chen et al. (2006). After preparing the protein sample into a certain mass concentration (w/v) and stirring it evenly, put it into the polypropylene vacuum bag, evacuate the bubbles (prevent bag breakage during high-pressure treatment), and then heat-seal the package under vacuum conditions. Check the sealing status of the high-pressure equipment. Place the vacuum bag with samples into the sample container of high-pressure equipment, set the pressure and pressure-maintaining time (pressure fluctuation range of ±10 MPa) from the computer, take it out after treatment, and then freeze and dry it for use. Prepare the solution with a mass concentration of 14% from the frozen and dried PPI using deionized water, heat it for 1 h at 95 °C, quickly cool it after taking it out, and determine the gel hardness, springiness, and cohesiveness using TA-TX2i texture instrument (probe diameter of 12 mm) after placing it for 24 h at 4 °C. Slightly modify it by the methods used by Pinterits and Arntfield (2008). Operating mode: TPA; pretest speed, 2.0 mm/s; test speed, 0.8 mm/s; pressing distance, 50%; posttest speed, 0.8 mm/s; data acquisition rate, 200/s. Gel hardness (g) = peak force in the first compression (Force 2); springiness = the ratio of the time taken from starting the second compression to ending the compression and the time taken from starting the first compression to ending the compression (time diff 4:5/time diff 1:2); cohesiveness = ratio of the areas under the positive peaks in the first and second compressions.

1. Pressure and time

The effects of different pressures and times on the curdlan hardness, springiness, and cohesiveness of PPI are shown in Figs. 7.1 and 7.2. It was shown from Fig. 7.1 that the hardness of curdlan formed by PPI increased first and then decreased with the increase of pressure. When the pressure was 100 MPa, the maximum hardness of gel formed by PPI was 172.52 g. Compared with other pressure levels, there was a significant difference ($p < 0.05$); when the pressure exceeded 100 Mpa, the hardness decreased sharply; it was shown from the impact of different pressures on gel springiness, within the range from 50 to 120 Mpa, that the gel springiness was high and larger than 0.7, but the change was not significant ($p > 0.05$), and the gel springiness decreased when the pressure exceeded 120 Mpa. It was shown from the figure that with the increase of pressure, the cohesiveness first increased and then decreased slightly and its value changed from 0.33 to 0.38, which was not significant ($p > 0.05$). The natural structures of most proteins were generally stabilized by the interaction of some non-covalent bonds. The high-pressure treatment might destroy the non-covalent bond balance of the protein, which would force the original structure of the protein to extend, and hydrogen bond, hydrophobic bond, ionic bond, and other non-covalent bonds changed, thus leading to the change in the properties of protein (Angsupanich et al. 1999). It is the reason why ultrahigh pressure can change the PPI curdlan. Another study showed that with the increase of pressure, the more complete the protein denaturation was, the more dense and

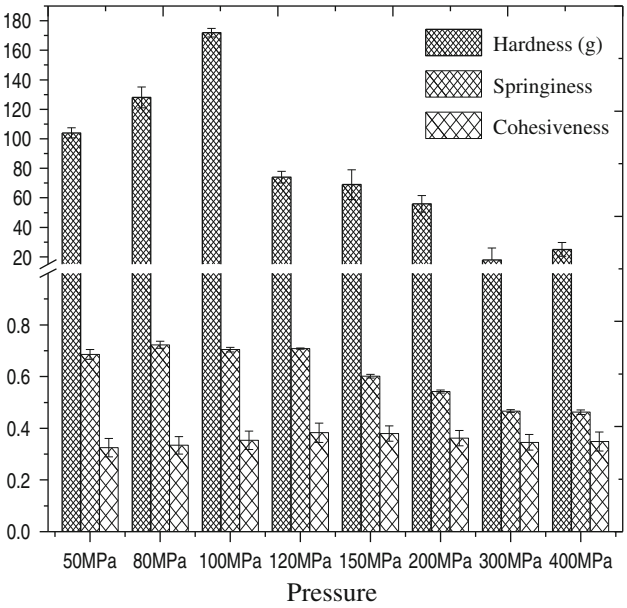

Fig. 7.1 Impact of pressure on the PPI curdlan

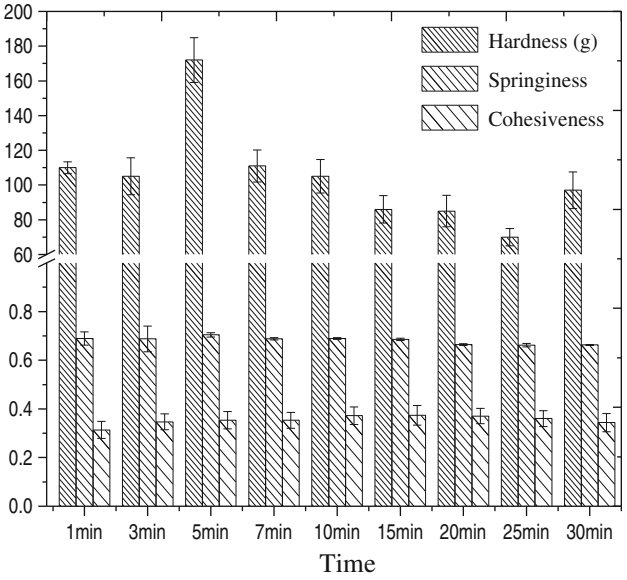

Fig. 7.2 Impact of treatment time on the PPI curdlan

fine the gel network formed by it, which might lead to the increase of gel hardness; however, after the pressure increased to a certain extent, the protein aggregation might occur, and its gelation would decrease. In this study, when the pressure was greater than 100 MPa, with the increase in pressure, protein aggregation might gradually increase, resulting in the significant decrease of hardness of curdlan formed.

It was shown from Fig. 7.2 that the effect of different treatment time on gel hardness was significant ($p < 0.05$), and the gel hardness value was highest after it had been processed for 5 min, and the hardness of PPI significantly reduced over time. With the gradual increase of time, the springiness and cohesiveness PPI gel first increased and then decreased slightly; the springiness reached the maximum value after it had been processed for 5 min, being 0.704; the cohesiveness reached the maximum value after it had been processed for 15 min, being 0.374. The ultrahigh-pressure treatment can enhance the aggregation of protein subunits; however, after the protein polymerization reached a certain extent, the effect on increasing protein polymerization was not obvious after continuing to increase the treatment time, and the dense and orderly gel network might be damaged and aggregation might be caused, and thus its gel hardness would significantly be reduced.

2. Protein concentration and pH

The effects of different protein concentrations and pH on the curdlan of PPI are shown in Figs. 7.3 and 7.4. It was shown in Fig. 7.3 that the gel hardness increased first and then decreased with the increase of the concentration of peanut protein, the gel hardness reached the maximum value when the concentration was 5%, and the gel hardness gradually decreased with the gradual increase of concentration; it was shown from the figure that with the gradual increase of concentration, the springiness and cohesiveness of PPI first increased and then decreased. The springiness reached the maximum value when the protein concentration was 10%, being 0.796; the cohesiveness reached the maximum value when the protein concentration was 15%, being 0.402; the protein concentration continued to increase to 20%; and cohesiveness dropped to 0.372. Under a certain pressure, with the increase of protein concentration, the nonbinding liquid of protein solution with high concentration decreased, and the strength of gel formed was higher than that of protein solution with a low concentration; when the concentration was very large, the gel was difficult to form a dense and orderly network structure, so the strength would be reduced (Briscoe et al. 2002; Gosal and Ross-Murphy 2005).

It was shown from Fig. 7.4 that the pH value had a great effect on the strength and springiness of the gel. The gel hardness reached the maximum value when the PH was 4.2, being 172.52 g, decreased to 10.56 g when pH was 6.8, and then increased to 46.33 g when pH was 8.3; however, it decreased to 7.67 g when pH increased to 10.3; the gel springiness was good when pH was 4.2, decreased to 0.60 when pH increased to 6.8, reached the maximum value of 0.78 when pH was 8.3, and decreased to 0.59 when pH was 10.3. The change trend of cohesiveness was completely different from that of hardness and springiness. With the gradual

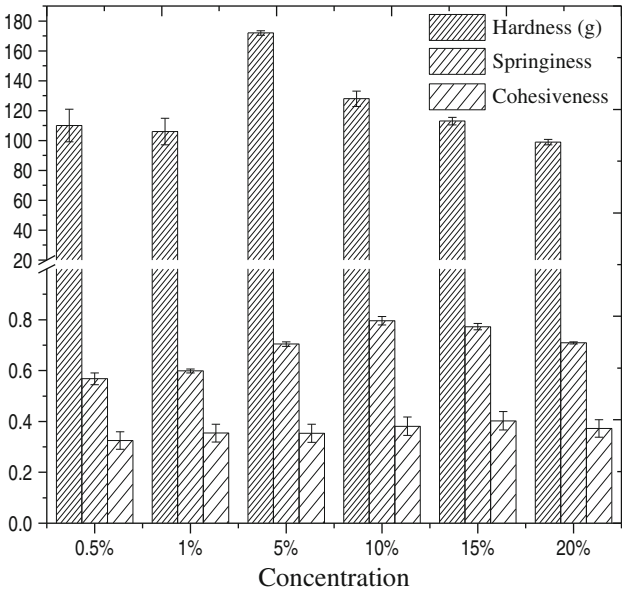

Fig. 7.3 Impact of protein concentration on the PPI curdlan

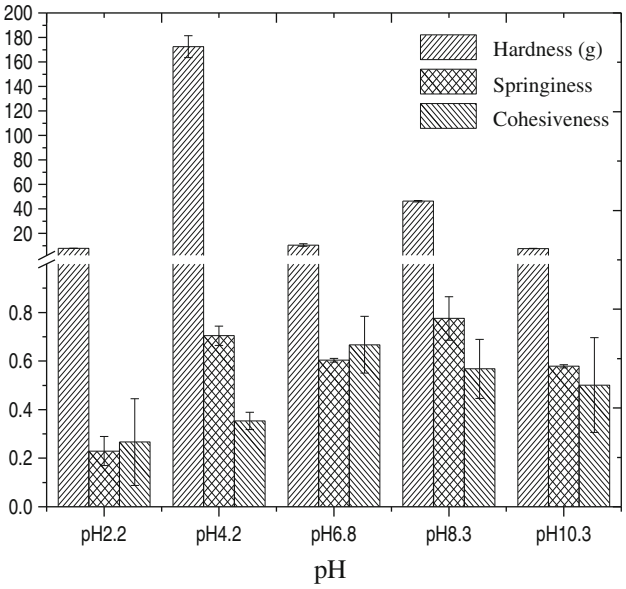

Fig. 7.4 Impact of pH on the PPI curdlan

increase of pH value, the cohesiveness of PPI increased first and then decreased and reached the maximum value at neutral pH conditions, being 0.667. It was shown from the impacts of pH on the hardness, springiness, and cohesiveness of PPI gel that it was more favorable for the formation of curdlan when it was in the vicinity of the isoelectric point, because when pH was close to the isoelectric point, the attractive force was greater than repulsive force, the protein conformation was compact, and a compact gel network was formed; when pH was at the non-isoelectric point, the force between the molecules was repulsive, the spatial conformation was relatively loose, and the structural strength of formed gel network was low. It was shown from the experimental results that the curdlan formed by PPI had good hardness and springiness at the same time when the pH value was 4.2. Therefore, optimization would be conducted when the pH value was 4.2 in the latter processes.

From the above single-factor results, the impact of ultrahigh pressure on the springiness and cohesiveness of PPI curdlan was not large, being within the variation ranges of 0.23–0.78 and 0.26–0.67, respectively. Ultrahigh pressure had a large impact on its hardness, being within the variation range of 18–172.52 g, so this book will optimize the formation process of PPI curdlan by taking gel hardness as an indicator.

1.2 Box-Behnken Combination Design Test

According to the results of single-factor test, Box-Behnken combination design was conducted to pressure, time, and protein by taking gel hardness as the evaluation index (Table 7.1) (Xu 1997) to further evaluate the interaction of pressure, time, and protein concentration on the gel hardness and optimize its process. Test was conducted according to Box-Behnken combination design program; see Table 7.2 for test combination and results.

According to the results of Table 7.2, the regression coefficients were calculated to establish the mathematical regression model between PPI curdlan hardness and the three factors of pressure, time, and concentration.

X_1, X_2, and X_3 represent the pressure, time, and concentration, respectively. The variance analysis of test results is shown in Table 7.3.

The variance analysis significance test results showed that the regression coefficient of the model was $P = 0.000918$ ($p < 0.01$), indicating that the regression was significant, and $R^2 = 0.9771$ in the model, indicating that the model was in good agreement with the actual test, and there was a significant linear relationship between independent variable and response value, and it could be predicted using the theory of PPI curdlan test after ultrahigh-pressure treatment. After removing the nonsignificant items at the significance level of $p = 0.05$, the optimized equation is

Table 7.1 Box-Behnken combination design test level

Canonical variate Z	Pressure (X_1)/MPa	Time (X_2) min	Concentration (X_3)/%
Upper level (1)	200	10	10
Zero level (0)	100	5	5
Lower level (−1)	50	3	1

Table 7.2 Experimental design and results

Treatment number	X_1 pressure (MPa)	X_2 time (min)	X_3 concentration (%)	Hardness (g)
1	−1(50)	−1(3)	0(5)	84.60
2	−1(50)	1(10)	0(5)	95.95
3	1(200)	−1(3)	0(5)	35.12
4	1(200)	1(10)	0(5)	62.26
5	0(100)	−1(3)	−1(1)	93.56
6	0(100)	−1(3)	1(10)	141.43
7	0(100)	1(10)	−1(1)	101.28
8	0(100)	1(10)	1(10)	126.43
9	−1(50)	0(5)	−1(1)	104.70
10	1(200)	0(5)	−1(1)	34.61
11	−1(50)	0(5)	1(10)	131.94
12	1(200)	0(5)	1(10)	71.79
13	0(100)	0(5)	0(15)	173.20
14	0(100)	0(5)	0(5)	169.24
15	0(100)	0(5)	0(5)	176.45

$$Y = 172.9633 - 26.67625X_1 + 17.18X_3 - 66.69792X_1X_1 - 36.782928X_2X_2 - 20.5054X_3X_3 \quad (7.1)$$

1. Interaction Effect Between Test Factors

The response surfaces of interactions of treatment time and protein concentration, treatment pressure and protein concentration, as well as pressure and time on the hardness of PPI curdlan are shown in Figs. 7.5, 7.6, and 7.7. It was shown from the figures that when the pressure, time, and concentration were low, the hardness of PPI curdlan increased with the increase of pressure, time, and concentration; when the pressure, time, and concentration were high, the hardness of PPI curdlan decreased with the increase of pressure, time, and concentration. When the pressure, time, and concentration were close to the central values, the hardness of curdlan reached the maximum value; when the factors deviated from the central values, the farther the deviation distance was, the lower the hardness of curdlan was, and the factors have secondary effect on the response value.

Table 7.3 Regression analysis results

Source	DF	SS	MS	F	Pr > F	Significance analysis
X_1	1	5692.979	5692.979	49.57911	0.000892	**
X_2	1	121.758	121.758	1.060368	0.350344	
X_3	1	2361.219	2361.219	20.56343	0.006199	**
X_1*X_1	1	16425.64	16425.64	143.0479	0.0001	**
X_1*X_2	1	62.33102	62.33102	0.542829	0.494358	
X_1*X_3	1	24.7009	24.7009	0.215116	0.662278	
X_2*X_2	1	4995.629	4995.629	43.50602	0.001204	**
X_2*X_3	1	129.0496	129.0496	1.123869	0.337589	
X_3*X_3	1	1552.512	1552.512	13.52055	0.014338	*
Model	9	29180.95	3242.328	F1 = 28.23684	0.000918	**
Error	5	574.1308	114.8262			
(Lack of fit)	3	548.0547	182.6849	F2 = 14.01169	0.067348	not significant
(Pure error)	2	26.07607	13.03803			
Total	14	29755.08				

*Represents significance at the level of 0.05, and **represents the significance at the level of 0.01

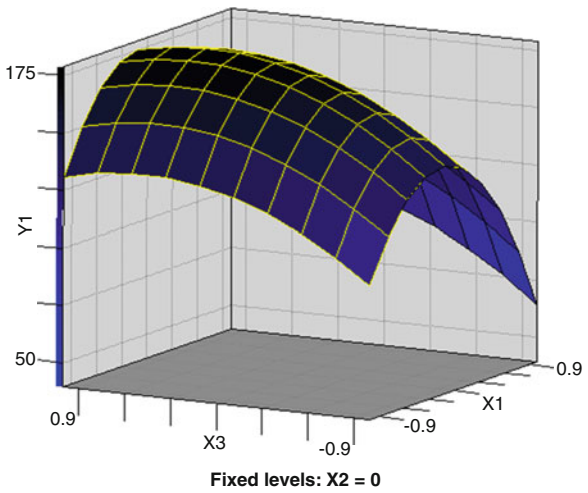

Fig. 7.5 Interaction of pressure and protein concentration on the hardness of PPI curdlan

2. Importance of factors

Analyze the importance of factors by contribution rate method:

$$\delta = \begin{cases} 0 & \text{If } F \leq 1 \\ 1 - 1/F & \text{If } F \leq 1 \end{cases} \tag{7.2}$$

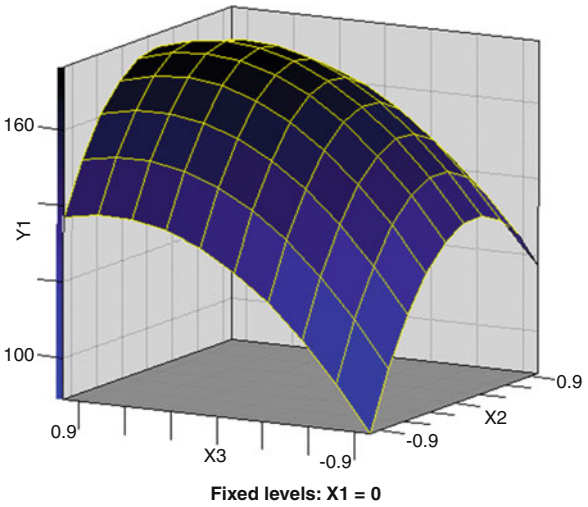

Fig. 7.6 Interaction of time and protein concentration on the hardness of PPI curdlan

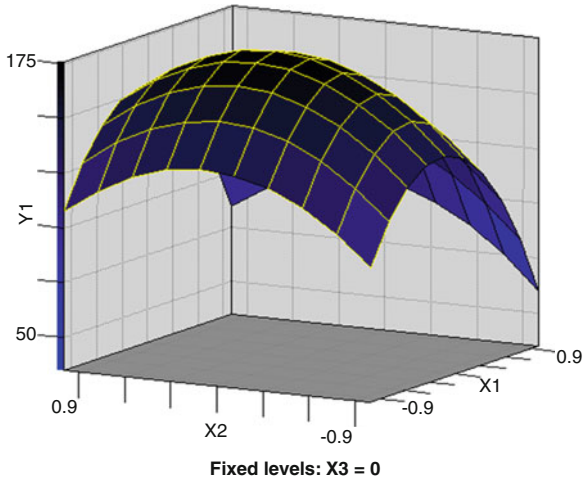

Fig. 7.7 Interaction of pressure and time on the hardness of PPI curdlan

Assume that the mean square ratio of significance test of regression coefficients are $F(j)$, $F(ij)$, and $F(jj)$.

The contribution rate of each factor to the index was expressed as

$$\Delta_j = \delta_j + \frac{1}{2} \sum_{\substack{i=1 \\ i=j}}^{m} \delta_{ij} + \delta_{jj}, j = 1, 2, \ldots\ldots, m \tag{7.3}$$

where δ_j represented the standard conversion value of the F value of the j-th factor, δ_{ij} represented the standard conversion value of the F value of interaction between the i-th factor and the j-th factor, δ_{jj} represented the standard conversion value of the F value of the quadratic term of the j-th factor, and $\triangle_j$ represented the contribution size of the j-th factor to the extracted results.

According to the mean square ratio F in Table 7.3, it was shown that the contribution rates of pressure, time, and protein concentration to the hardness of gel were $\triangle_1 = 1.9728$, $\triangle_2 = 1.0891$, and $\triangle_3 = 1.9325$, respectively, because $\triangle_1 > \triangle_3 > \triangle_2$, the sizes of effects on the hardness of gel, were as follows: pressure> concentration of PPI > time.

3. Ultrahigh-Pressure Conditions

According to the mathematical analysis of regression model, the optimum technological parameters of PPI curdlan after ultrahigh-pressure treatment were pressure of 115 MPa, time of 5 min, and PPI concentration of 3.11%. The hardness of PPI gel was 176.96 g under this process condition. In order to further test the reliability of the response surface analysis method, the above optimal conditions were used for the ultrahigh-pressure treatment. The measured hardness of PPI gel was 174.37 g, and its relative error was small compared to the theoretical value, being 1.46%. Therefore, the ultrahigh-pressure condition parameters obtained by analysis and optimization using response surface were accurate and reliable, and they could be used for practical operation.

2 Physicochemical Characteristics

PPI is a kind of plant protein featuring rich sources, low price, high quality, and complete nutrition. Although natural PPI has a variety of functional characteristics, it cannot fully meet the actual production needs during the actual applications. In addition, when using PPI in the food industry as a food additive, it often needs to use several functional characteristics of protein. For example, during the treatment to add PPI to ham, not only the gelation of PPI is used, but also good water-binding capacity and oil-binding capacity of PPI are required. It is necessary to further study whether the changes in the water-binding capacity, oil-binding capacity, grain size, amino acid type, and content of PPI can be obtained properly after gaining the PPI with good gelation by ultrahigh-pressure physical method. Because of the action of a large number of hydrogen bonds, hydrophobic bonds, van der Waals force, ionic bonds, and coordination bonds in peanut protein molecules, the emulsification and solubility of peanut protein can be improved properly under a certain pressure. After making clear the change law of PPI gel characteristics during the ultrahigh-pressure treatment, this book has systematically studied other physicochemical characteristics of PPI, to provide a theoretical support to the actual applications of PPI.

2.1 Water-Binding Capacity and Oil-Binding Capacity

The water-binding capacity of protein is an indicator to evaluate the ability of protein products to absorb water. The water-binding capacity of protein plays a major role in the texture of the food, especially meat and baked dough; insoluble protein may cause swelling and result in the changes in volume after absorbing water. In addition, the rheological characteristics of the system may be affected (Zhou 1999). The oil-binding capacity of protein refers to the capacity of protein to absorb oil, and it plays a very important role in the formula and treatment of meat products, dairy products, sandwich biscuit, and other foods. For example, in chopped meat products, it can reduce the weight loss during cooking and help to maintain the stability of the shape (Maruyama et al. 1998).

The change laws of water-binding capacity and oil-binding capacity of PPI after ultrahigh-pressure treatment at different pressures, times, and protein concentrations are shown in Figs. 7.8, 7.9, and 7.10. It was shown from Fig. 7.8 that the water-binding capacity and oil-binding capacity of PPI after pressure treatment significantly increased ($p < 0.05$). With the increase of pressure, the water-binding capacity and oil-binding capacity increased gradually; under different pressure (50–200 MPa) treatment conditions, the oil-binding capacities of PPI increased by 45.98%, 43.65%, 50.01%, 50.31%, and 59.66%, respectively, and the water-binding capacities increased by 1.48%, 2.09%, 7.33%, 9.51%, and 29.46%, respectively. It was shown from the figure that the improvement of oil-binding capacity was more obvious than that of water-binding capacity. The water-binding capacity and oil-binding capacity of protein solution with a certain concentration gradually increased with the increase of pressure after ultrahigh-pressure treatment. This was because the high-pressure treatment might destroy the non-covalent bond balance of the protein, force globular protein molecules to extend, and expose the disulfide group, hydrophobic group, and other functional groups in molecular chain originally, and thus the water-binding capacity and oil-binding capacity of protein would gradually increase.

Figure 7.9 showed that with the extension of ultrahigh-pressure treatment time, the water-binding capacity and oil-binding capacity of PPI increased first and then decreased. The water-binding capacity reached the maximum value when the treatment time was 5 min, being 2.40 g/g; the oil-binding capacity reached the maximum value when the treatment time was 3 min, being 3.73 mL/g. Oil-binding capacity can play a role in both promoting and controlling fat absorption. In many food and biological systems, there is an interaction between proteins and lipids, which is not due to covalent bonds but the hydrophobic interaction between the nonpolar aliphatic chains of lipids and nonpolar regions of proteins. The energy of interaction between protein and lipid is lipid, especially the length of its aliphatic chain and hydrophobicity function of the protein. If the amino acids that constitute protein have a high average hydrophobicity, such protein can often strongly interact with lipids to form lipid-protein complex, which may change the structure of protein. The milk film formed when heating soybean milk is a kind of

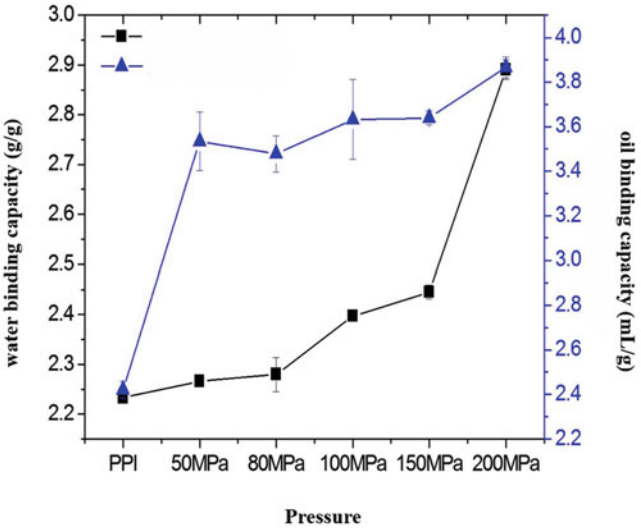

Fig. 7.8 Impact of different pressures on water-binding capacity and oil-binding capacity. ■ Water binding capacity; ▲ Oil binding capacity

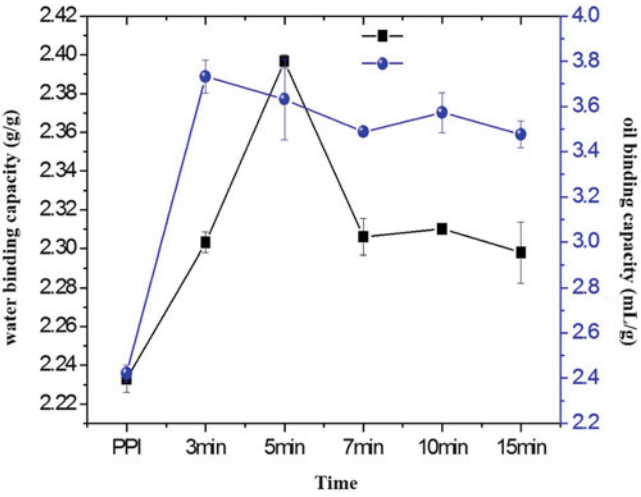

Fig. 7.9 Impact of different times on water-binding capacity and oil-binding capacity. ■ Water binding capacity; ● Oil binding capacity

lipid-protein complex. In this study, after a certain time of treatment, when the surface hydrophobicity index of protein increased, the side chain in the molecule was dissociated and opened, thus increasing the water-binding capacity and oil-binding capacity of protein; when the treatment time was prolonged, the protein was denatured, the structure became dense, and insoluble proteins increased, thus gradually decreasing the water-binding capacity and oil-binding capacity.

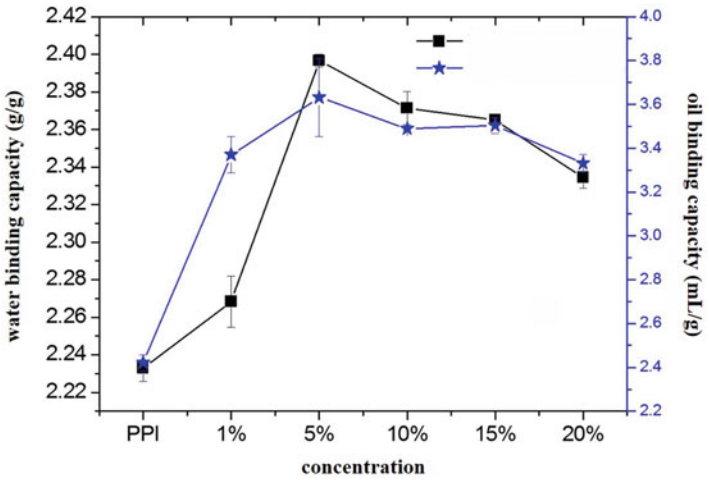

Fig. 7.10 Impact of different concentrations on water-binding capacity and oil-binding capacity. ■ Water binding capacity; ★ Oil binding capacity

It was shown from Fig. 7.10 that the water-binding capacity and oil-binding capacity of PPI at different concentrations changed significantly after high-pressure treatment and first increased and then decreased. The water-binding capacity and oil-binding capacity reached the maximum values when the concentration was 5%, being 2.40 g/g and 3.63 mL/g, respectively. The action of absorption of fat by protein was another form of emulsification. Protein could form an emulsion and a gel matrix when being added to meat, to prevent the fat from moving to the surface. Therefore, it played a role in promoting fat absorption or combination, so as to reduce the loss of fat and juice during the treatment of the meat and maintain the stability of shape. The oil-binding capacity increased with the increase of protein, small particles of low-density protein powder were able to absorb or retain a large number of oil compared with high-density protein powder, and high-pressure homogenization could increase the phase interface, thereby enhancing the protein-lipid interaction degree. The protein part in protein solution was unfolded under the action of ultrahigh pressure and thus caused the exposure of hydrophobic groups, thereby enhancing the water-binding capacity and oil-binding capacity. When the concentration of the protein solution was too high, the hydrophobic group could not be fully unfolded under the ultrahigh-pressure treatment, and then the protein was denatured and its structure became dense, resulting in a decrease in water-binding capacity and oil-binding capacity (Shi Yanguo and Sun Bingyu 2005).

In order to compare the functional characteristics of commercial soybean protein isolates, five kinds of soy protein isolates that were mainly produced and sold at home and abroad were bought. Among them, SPI emulsion type 1 and SPI injection type 1 were domestic commercial soybean protein isolates, and SPI emulsion type 2, SPI injection type 2, and SPI dissolution type were commercial soy protein isolates from Japan. The functional characteristics of each SPI were measured and compared with that of PPI under optimal ultrahigh pressure (115 MPa, 5 min,

Table 7.4 Comparison of functional characteristics of PPI and SPI

Type of protein	Oil-binding capacity (g/g)	Water-binding capacity (ml/g)	Gel hardness (g)	Springiness
SPI emulsion type 1	2.3563 ± 0.03^{b}	3.4027 ± 0.118^{f}	82.08	0.9686
SPI injection type 1	2.3259 ± 0.02^{c}	6.2657 ± 0.47^{e}	97.59	0.9744
SPI emulsion type 2	2.2268 ± 0.04^{d}	5.7216 ± 0.175^{d}	38.99	0.7603
SPI injection type 2	2.1593 ± 0.01^{e}	7.0698 ± 0.04^{c}	45.64	0.9674
SPI dissolution type	2.6790 ± 0.05^{f}	1.8755 ± 0.01^{b}	no gel	–
PPI after ultrahigh-pressure treatment	3.6318 ± 0.01^{a}	2.3965 ± 0.01^{a}	174.37	0.7332
PPI without treatment	2.421 ± 0.01^{b}	2.233 ± 0.02^{a}	115.81	0.7484

The same letter means that the difference is not significant ($p > 0.05$), and different letters mean that the difference is significant ($p < 0.01$)

3.11%) and PPI without ultrahigh-pressure treatment. The results are shown in Table 7.4. It was shown from the figure that the water-binding capacities of five commercial soybean isolates were significantly higher than that of PPI ($p < 0.01$) except SPI dissolution type, including PPI after ultrahigh-pressure treatment and PPI without ultrahigh-pressure treatment. There was no significant difference in the water-binding capacities of two PPIs ($p > 0.05$). However, the oil-binding capacity of PPI after high-pressure treatment was not only higher than that of natural PPI ($p < 0.01$) but also the commercial soy protein isolates ($p < 0.01$). There was no significant difference between the PPI without high-pressure treatment and domestic SPI emulsion type 1 ($p > 0.05$), and it is very significantly different from other types of SPI ($p < 0.01$). After comparison of the hardness of gel formed by various proteins, the hardness of curdlan formed by PPI after ultrahigh-pressure treatment was significantly higher than that of commercial soy protein isolate and PPI without high-pressure treatment ($p < 0.01$). It was shown from the figure that a certain ultrahigh-pressure treatment could improve the oil-binding capacity and gelation of PPI, and it was significantly higher than that of commercial soy protein isolate ($p < 0.01$), but its water-binding capacity was far less than that of commercial soy protein isolate ($p < 0.01$).

2.2 Molecular Weight Distribution

Figure 7.11 showed the molecular weight distribution diagrams of the PPI not treated at high pressure and the samples that had been treated for 5 min at 50, 100, and 200 MPa, respectively. The diagrams were obtained at multi-angle laser light scattering instrument through analysis. Table 7.5 is the result obtained from the diagrams in Fig. 7.11 by analysis using the software in the instrument. It was shown from Fig. 7.11 and Table 7.5 that there were significant changes in the distribution of PPI molecular weight after treatment under different pressures. There were mainly two peaks in the untreated protein: the peaks appeared at

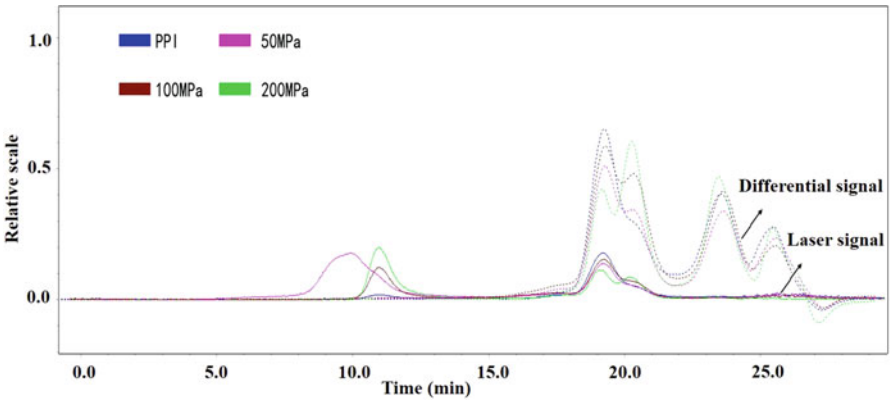

Fig. 7.11 Molecular weight distribution diagram of PPI after treatment at different pressures

Table 7.5 Molecular weight distribution result of PPI at different pressures

Sample	First peak (component)		Second peak (component)		Third peak (component)	
	Mw (Da)	Proportion (%)	Mw (Da)	Proportion (%)	Mw (Da)	Proportion (%)
Contrast	$3.648e^5$	70.87	$2.327e^5$	29.13	–	–
50 MPa	$3.762e^5$	60.44	$3.529e^5$	38.30	$6.292e^7$	1.27
100 MPa	$3.439e^5$	54.32	$2.133e^5$	45.68	–	–
200 MPa	$3.528e^5$	36.08	$1.861e^5$	62.95	$3.665e^7$	0.98

18.083–20.013 min and 20.073–21.585 min, respectively; the molecular weights were $3.648e^5$ Da component (I) and $2.327e^5$ Da component (II), respectively; and the contents were 70.87 % and 29.13%, respectively. After the high-pressure treatment, the component (I) was gradually decomposed. Under the pressure of 50 MPa, 100 MPa, and 200 MPa, it was shown that the peak appearance time and molecular weight of each sample component were basically the same as that of the samples without pressure treatment. However, the proportions of the components in the entire protein changed significantly. Component (I), namely, the main peak with large molecular weight, decreased obviously, and the content decreased to 36.08% at 200 MPa, which was half of that before treatment; component (II) showed a significant increase trend, and the components with larger molecular weight appeared at 50 MPa and 200 MPa, but the content was small, being about 1%. The above results showed that the pressure broke the weak sub-key bonds between the polypeptide chains in PPI, resulting in a decomposition of the components with a large molecular weight and the content of the components with a small molecular weight increased. However, under a certain pressure, a small amount of polymer might be formed in the protein at a certain pressure.

Figure 7.12 showed the molecular weight distribution diagrams of the PPI not treated at high pressure and the samples that had been treated for 3 min, 5 min, and 15 min at 100 MPa, respectively. The diagrams were obtained at multi-angle laser

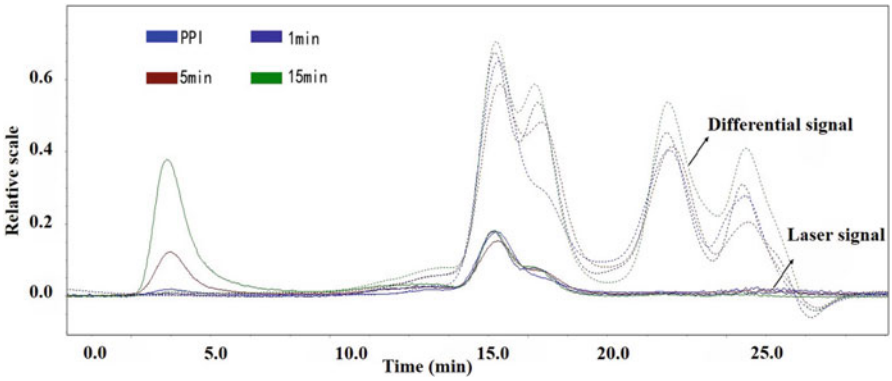

Fig. 7.12 Molecular weight distribution diagram of PPI after treatment for different times

light scattering instrument through analysis. Table 7.6 showed the result obtained from the diagrams in Fig. 7.12 by analysis using the software in the instrument. It was shown from Fig. 7.12 and Table 7.6 that there were significant changes in the distribution of PPI molecular weight after treatment for different times under a certain pressure. The peaks of samples appeared at 18.032–20.013 min and 19.735–21.715 min. Compared with the samples without pressure treatment, most of the components with a large molecular weight (the peak appeared at 18.032–20.013 min) were decomposed, and the contents of the components with a small molecular weight (peak appeared at 19.735–21.715 min) increased obviously. When the time reached 15 min, new polymer appeared in the sample, the peak appeared at 10.044–12.113 min, the molecular weight was $5.667e^7$ Da, and the content was 1.31%. With the increase of treatment time, the components with a large molecular weight were decomposed first quickly and then slowed down. At 5 min, the content of components with a large molecular weight was 54.32%, which was higher than that of samples at 3 min (52.54%) and 15 min (49.96%); the content of components with a small molecular weight was 45.68%, which was lower than that of samples at 3 min (47.46%) and 15 min (48.72%). Compared with the pressure effect (result in Table 7.5), the effect of time was significantly weaker than that of pressure under the same external environment.

Figure 7.13 showed the molecular weight distribution diagrams of the PPI not treated at high pressure and the PPIs with a concentration of 1% (w/v), 5% (w/v), and 20% (w/v), respectively, after treatment at 100 MPa. The diagrams were obtained at multi-angle laser light scattering instrument through analysis. Table 7.7 showed the result obtained from the diagrams in Fig. 7.13 by analysis using the software in the instrument. It was shown from Fig. 7.13 that the peaks of samples appeared at 18.083–20.013 min and 19.738–21.715 min. It was shown from Table 7.7 that compared with the PPI not treated at high pressure, the content of the component with a large molecular weight (the peak appeared at 18.083–20.013 min) decreased sharply first and then gradually increased with the increase of concentration; the content of the component with a small molecular weight (the peak appeared at 19.738–21.715 min) increased sharply first and then

Table 7.6 Molecular weight distribution result of PPI after treatment for different times

Sample	First peak (component)		Second peak (component)		Third peak (component)	
	Mw (Da)	Proportion (%)	Mw (Da)	Proportion (%)	Mw (Da)	Proportion (%)
Contrast	$3.648e^5$	70.87	$2.327e^5$	29.13	–	–
3 min	$1.023e^5$	52.54	$1.412e^5$	47.46	–	–
5 min	$3.439e^5$	54.32	$2.133e^5$	45.68	–	–
15 min	$3.439e^5$	49.96	$2.169e^5$	48.72	$5.667e^7$	1.31

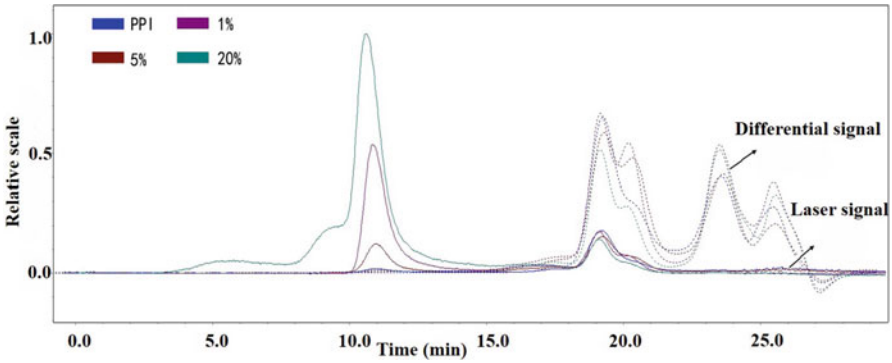

Fig. 7.13 Molecular weight distribution diagram of PPI with different concentrations after ultrahigh-pressure treatment

Table 7.7 Molecular weight distribution result of PPI with different concentrations after ultrahigh-pressure treatment

Sample	First peak (component)		Second peak (component)	
	Mw (Da)	Proportion (%)	Mw (Da)	Proportion (%)
Contrast	$3.648e^5$	70.87	$2.327e^5$	29.13
1%	$3.286e^5$	52.18	$1.723e^5$	47.82
5%	$3.439e^5$	54.32	$2.133e^5$	45.68
20%	$3.491e^5$	65.41	$1.883e^5$	34.59

gradually decreased with the increase of concentration. When the concentration was 1–5%, the molecular weight distribution was in a relatively stable state without obvious changes, and the content change of the two components was only 2.14%; when the concentration was greater than 5%, the content change of the two components increased to 11.09%. The result above was significantly different from the result of the impact of pressure and time on the molecular weight distribution of PPI. This indicated that during the ultrahigh-pressure processing, the impacts of different treatment conditions on the molecular weight distribution

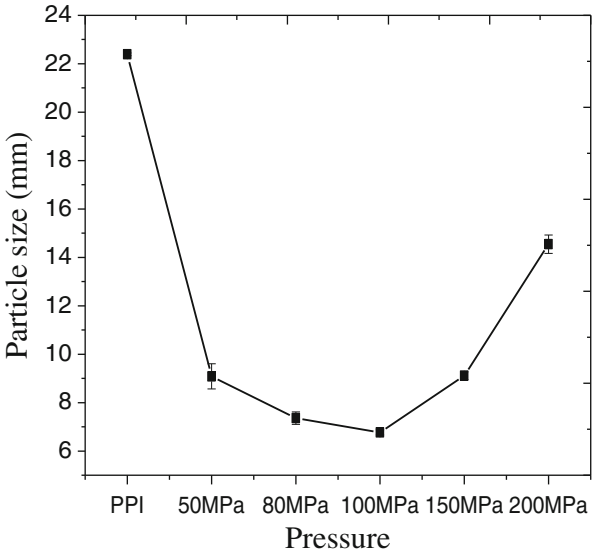

Fig. 7.14 Impact of different pressures on the particle size of PPI

of PPI were completely different, which resulted in completely different of texture characteristics after the formation of curdlan (Figs. 7.1, 7.2, and 7.3). It was known after further analysis that when the contents of the two components in the sample accounted for 50%, respectively, the texture of the curdlan formed was good, and the large polymers in the sample could not improve the texture characteristics of the curdlan formed.

2.3 Particle Size

The particle sizes of the samples are shown in Figs. 7.14, 7.15, and 7.16. It was found that the average particle size of PPI after ultrahigh-pressure treatment drastically changed. Figure 7.14 showed the impacts of different pressures on the particle size of PPI. It was shown from the figure that the average particle size of untreated PPI was 22.39 μm, and the average particle sizes after treatment at different pressures were 9.08 μm at 50 MPa, 7.36 μm at 80 MPa, 6.77 μm at 100 MPa, 9.11 μm at 150 MPa, and 14.55 μm at 200 MPa, respectively. The average particle size of PPI greatly decreased after modification by high-pressure treatment and reached the minimum value at 100 MPa. The average particle size decreased by 15.62 μm compared to that before treatment; however, with the further increase of pressure, the average particle size begun to increase, which was consistent with the impact of dynamic ultrahigh-pressure micro-jet technology on the particle size of water-in-oil emulsions in the research of Jafari et al. (2007). The particle size decreased sharply at a low pressure, and it showed an increase trend at a high pressure. There are two different interpretations of this result. One explanation is that after pressure treatment, the final particle size of the substance

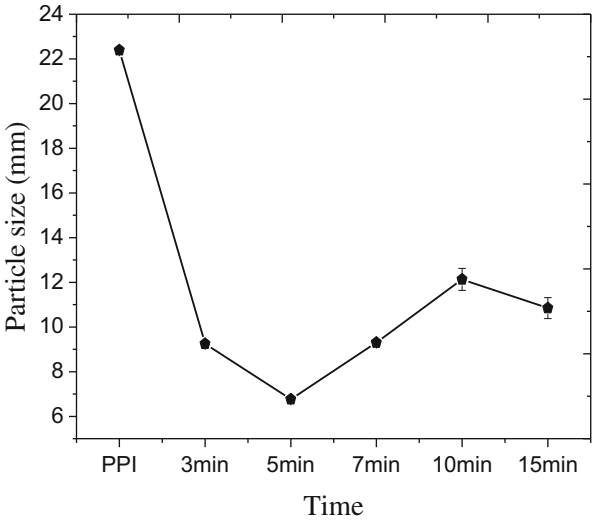

Fig. 7.15 Impact of different times on the particle size of PPI

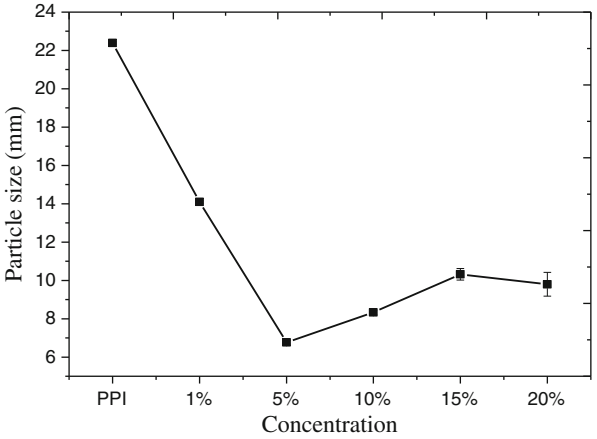

Fig. 7.16 Impact of different concentrations on the particle size of PPI

depends on the competition results of two opposing factors of particle fragmentation and particle reaggregation. When the protein polymer is broken into smaller polymers, a new surface is formed, and the new polymers tend to reaggregate due to the thermodynamical instability. If reaggregation dominates, the particle size will increase. The other explanation is that this result is caused by "overpressure" (Kolb et al. 2001; Desrumaux and Mareand 2002). When the pressure increases, the water will be compressed, and its temperature will increase. It is generally believed that under the adiabatic conditions, the temperature at 20 °C will increase by 3 °C after applying 100 MPa each time; therefore, the possibility of reaggregation will be raised, and thus the particle size will be increased.

Figure 7.15 showed the changes of the particle size of PPI after treatment for different times. It was shown from the figure that with the extension of the treatment

time, the particles were broken and the particle size decreased rapidly and reached the minimum value at 5 min; with the continuous extension of treatment time, some tiny protein particles recombined to form new polymers, and thus the particle size increased. Figure 7.16 showed the impacts of different protein concentrations on the particle size of PPI. It was shown from the figure that among the protein solutions with different concentrations, after a certain high-pressure treatment, the protein particles became smaller; the average particle size reached the minimum value when the concentration was 5%, being 6.77 μm; when the concentration continued to increase, the PPI with a small particle size formed a new polymer and thus led to reaggregation within the limited solution space scope, and the particle size slowly increased.

2.4 Microscopic Morphology

1. SEM scanning of ultra-high pressure PPI samples

The electron microscopic scanning diagrams of the samples are shown in Fig. 7.17, which are obtained in the magnification of 10,000 times. A in the figure is PPI not treated at ultrahigh pressure; B–F are PPI after treatment at 50, 80, 100, 150, and 200 MPa, respectively; G–J are the samples of PPIs with a concentration of 1%, 10%, 15%, and 20% (w/v), respectively, after treatment for 5 min at 100 MPa; and K–N are the samples of PPIs after treatment for 3, 7, 10, and 15 min, respectively, at 100 MPa.

As shown in Fig. 7.17a, the surface of the original sample of untreated PPI was visibly viscous and smooth, and the protein particles were clustered together with compact structure and free of obvious pores; after the treatment at the pressure of 50 MPa (Fig. 7.17b), the polymer of PPI was broken, the polymer surface was not smooth and the viscosity became smaller, and there were some small pores. When the pressure reached to 80 MPa (Fig. 7.17c), due to the intensified degree of crushing, protein polymer was decomposed into countless irregular small particles under high-pressure mechanical force, and when they would combine together closely, the pores become large, but the surface was not visibly viscous. When the pressure increased to 100 MPa (Fig. 7.17d), the surface of the sample became slightly viscous; its viscosity was between the values in Fig. 7.17b, c. A small amount of spherical particles were combined together, with visible uniform pores. With the further increase of pressure, the peanut globulin particles should be further broken into smaller particles under high pressure conventionally; however, this change trend was not intensified, the size of peanut protein particles became large, and most of them were in the form of sheets. This could be confirmed using the electron microscope scanning diagrams after treatment at 150 MPa and 200 MPa, respectively (Fig. 7.17e, f). The spherical particles in the sample of Fig. 7.17e almost completely disappeared, and the surface was very viscous and in the form of sheets, but there were a small number of larger visible pores, while the spherical

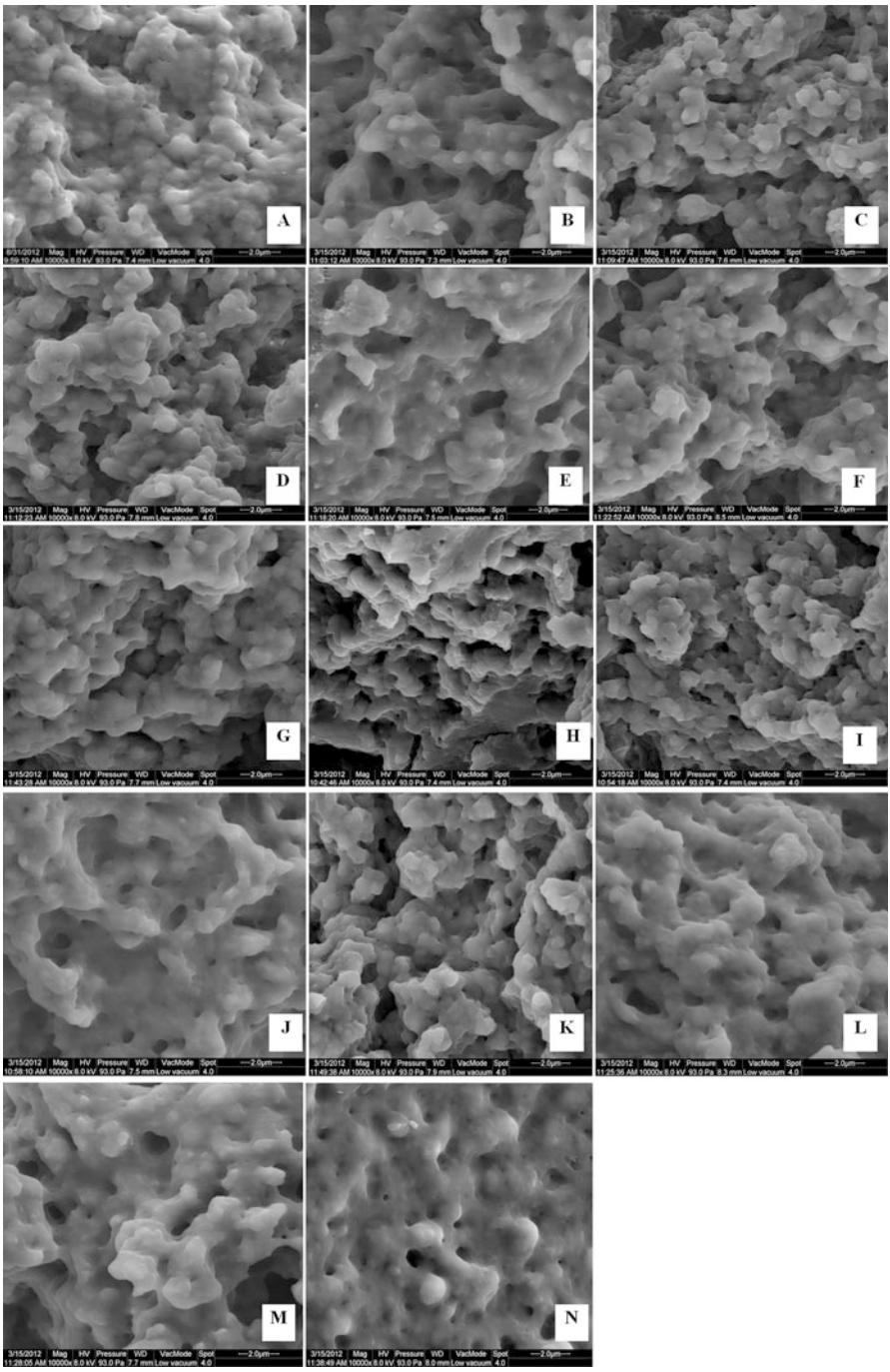

Fig. 7.17 SEM scanning diagrams of PPI samples before and after ultrahigh-pressure treatment (10,000×)

particles in the sample of Fig. 7.17f were incomplete with large pores. The possible explanation is that on the one hand, the large particles continued to rupture; on the other hand, small particles were aggregated into large particles, and the aggregation was predominant, so the particle size became large at large treatment pressures (>100 MPa). The above results showed that the pressure could break the peanut globule protein particles, making its structure become loose; with the increase of treatment pressure, the degree of crushing was intensified and became the most severe at 100 MPa. At this time, the particle size of peanut globule was the smallest, and the surface was uneven; after continuing to apply pressure, the specific surface area of particle increased, the aggregation became dominant, and the particle size increased, which was very consistent with the particle size change of the peanut protein at different pressures measured in Fig. 7.11.

It was shown from Fig. 7.17g–j that there were spherical particles on the surface of PPI with a low concentration (Fig. 7.17g); with the increase of concentration, the spherical particles in the protein disappeared, and protein particles were broken into flaky substances at the concentration of 10% (Fig. 7.17h); however, after continuing to increase the concentration to 15% (Fig. 7.17i), clustered substances appeared at the surface of protein; after the concentration reached 20% (Fig. 7.17j), the sample became viscous visibly without obvious pores. This was consistent with the results of particle size change of PPI at different concentrations in Fig. 7.12. Figure 7.17k–n were the electron microscope scanning diagrams of samples after different times. It was shown from the figures that at a certain pressure (100 MPa), there were obvious spherical particles on the surface of sample within a short time (5 min); however, with the extension of time, the viscosity at the surface of sample increased obviously, and pores decreased obviously.

2. SEM scanning of curdlan samples formed by PPI after ultra-high pressure treatment

Figure 7.18a–h in Fig. 7.18 are the diagrams of curdlan formed by PPI. They were obtained using scanning electron microscopy at 10,000 times. Among them, Fig. 7.18a is the electron microscopy diagram of curdlan formed by PPI not treated at ultrahigh pressure, and Fig. 7.18b–h are the electron microscopy diagrams of curdlans formed by PPI after the treatment at 50 MPa, 100 MPa, 200 MPa, 1% (w/v), 20% (w/v), 3 min, and 15 min, respectively. The microstructures of the gels formed by various samples were significantly different. It was shown from Fig. 7.18a that there were many small pores in the curdlan formed by PPI not treated at high pressure, and protein particles were connected compactly and densely. In the curdlan formed after treatment at 50 MPa, the protein particles were connected together in clusters, and the pores became obviously large (Fig. 7.18b); in the curdlan formed after treatment at 100 MPa, globular protein particles were compactly connected together in clusters or strips (Fig. 7.18c); in the curdlan formed after treatment at 200 MPa, although protein particles were tightly connected together, they did not form the original globular structure (Fig. 7.18d). It was shown from Fig. 7.18e that the parts at the surface of sample were clustered and the structure was not compact with visible large pores. It was shown from Fig. 7.18f

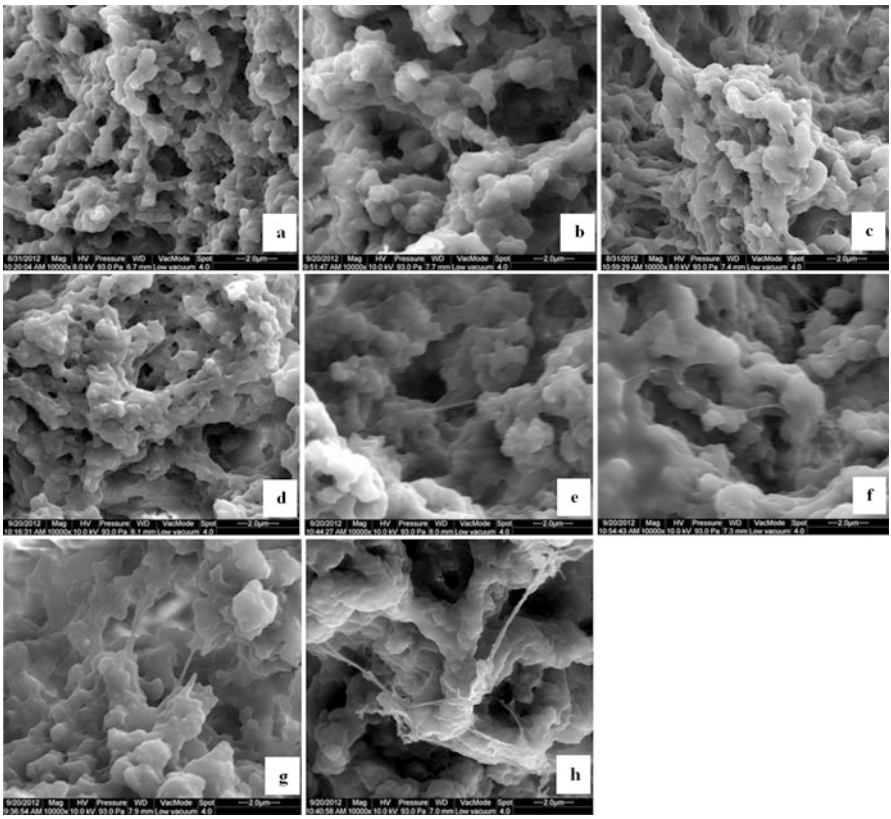

Fig. 7.18 SEM scanning diagrams of curdlan formed by PPI samples before and after ultrahigh-pressure treatment (10,000×)

that the curdlan formed by sample obviously increased, and protein particles formed the cluster structure which was not compact but viscous. For the microstructure of curdlan formed by the sample in Fig. 7.18g, there were a few of small pores at the surface of sample, most of the protein particles formed flakes, and a small part of them formed clusters. For the gel sample in Fig. 7.18h, the visible pores increased obviously, the spherical structure at the surface of sample disappeared, most of the spherical particles formed flake substances, but they did not connect together tightly, so there were many large pores. Compared with the microstructures of the samples before forming curdlan (Fig. 7.16), it was shown that ultrahigh-pressure treatment changed the microstructure of PPI and the microstructures of the curdlan formed by it were significantly different with the changes in pressure, time, and protein, which also led to significantly different texture characteristics of the curdlan formed by the samples (as shown in the results of 2.1.2). After further analysis, it was shown that there were obvious spherical particles at the surface of protein particle sample and a small amount of particles were

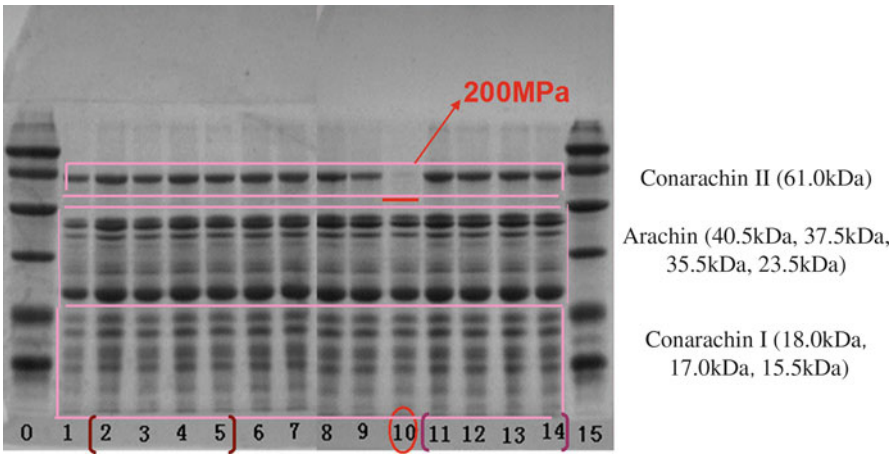

Fig. 7.19 SDS-PAGE analysis of PPI. Note: 0, 15: standard sample; 1: PPI; 2–5: 1%, 10%, 15%, 20%; 6–10: 50, 80, 100, 150, 200 MPa; 11–14: 3, 7, 10, 15 min

combined together to form a uniform pore structure (Fig. 7.18d), and the curdlan formed was in clustered and stripped microstructure (Fig. 7.18c), with good texture characteristics (Fig. 7.1). When the surface of protein appeared viscous or protein particles were closely gathered together, the texture characteristics of the curdlan formed were poor.

2.5 Protein Components and Bands

The SDS-PAGE electrophoretograms of PPI before and after ultrahigh-pressure treatment are shown in Fig. 7.19. The subunit bands of PPI were clearly shown in the figure, the molecular weights corresponding to the subunit bands were, respectively, 61.0 kDa, 40.5 kDa, 37.5 kDa, 35.5 kDa, 23.5 kDa, 18.0 kDa, 17.0 kDa, and 15.5 kDa. Among them, 61.0 kDa belonged to conarachin II; 40.5 kDa, 37.5 kDa, 35.5 kDa, and 23.5 kDa belonged to arachin; and 18.0 kDa, 17.0 kDa, and 15.5 kDa belonged to conarachin I (Prakash and Narasinga 1986). The solubilities of protein sample (according to the order in the figure) were $73.88 \pm 0.24\%$, $68.43 \pm 0.48\%$, $68.90 \pm 0.25\%$, $70.09 \pm 0.27\%$, $74.91 \pm 0.12\%$, $65.20 \pm 0.23\%$, $65.45 \pm 0.24\%$, $65.88 \pm 0.24\%$, $65.03 \pm 0.24\%$, $64.35 \pm 0.25\%$, $71.16 \pm 0.23\%$, $70.89 \pm 0.10\%$, $68.24 \pm 0.33\%$, and $67.75 \pm 0.08\%$, respectively.

From the solubilities of samples, the results of Fig. 7.19 were not due to the differences in the solubilities of samples but due entirely to the treatment at different ultrahigh pressures. It was shown after further analysis that compared with that of untreated PPI, the 61.0 kDa subunit bands at different times and in the samples with different protein concentrations did not have any obvious changes, except that the color got darker. With the increase of pressure, the color of 61.0 kDa

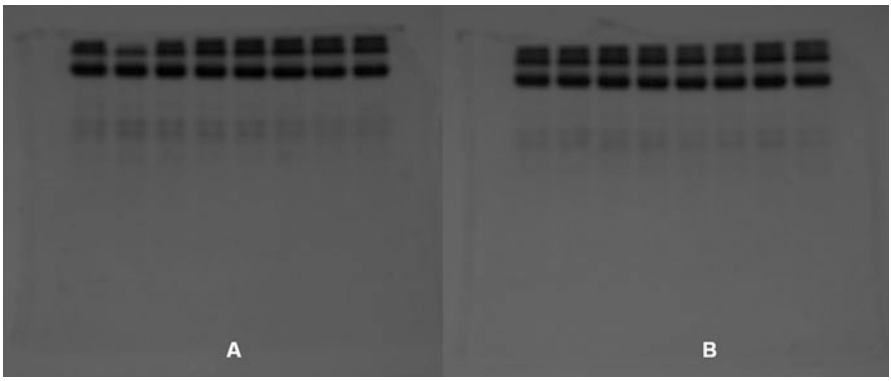

Fig. 7.20 Native PAGE analysis of PPI. Note: (**a**) from *left* to *right*, PPI, PPI2, 50 MPa, 80 MPa, 100 MPa, 150 MPa, 200 MPa, 3 min. (**b**) Samples from *left* to *right*: PPI, 7 min, 10 min, 15 min, 1%, 10%, 15%, 20%

subunit band first got darker and then lighter, showing that PPI first aggregated and then unfolded after ultrahigh treatment. After comparing the electrophoretic bands of PPI before and after ultrahigh-pressure treatment, it was found that there was no significant difference in the subunit bands of conarachin I, showing that ultrahigh-pressure treatment has no impact on conarachin I basically; after the treatment at different pressures, the subunit bands of PPI became darker obviously, showing that ultrahigh pressure caused aggregates in the arachin of PPI. Because β-mercaptoethanol was used in SDS-PAGE electrophoresis to break the disulfide bonds of PPI, the aggregate bonds showed that non-disulfide-covalent cross-linker was formed in PPI due to the effect of pressure. The above results indicated that conarachin II was most sensitive to pressure than arachin and conarachin I.

Figure 7.20 is the Native PAGE of PPI, corresponding to the nonreduction situation in Fig. 7.19. It was shown from the figure that at the top of the separation gel, each sample had three aggregates, being N I, N II, and N III, respectively. Figure 7.19 is the corresponding reduction situation. It was found after comparing Fig. 7.19 with Fig. 7.20 that the bands corresponding to N I, N II, and N III had appeared, showing that disulfide bonds played an important role in the aggregates of N I, N II, and N III. The difference among samples after treatment at different ultrahigh pressures was not reflected obviously in the figure.

2.6 Thermal Performance

1. Pressure

DSC is widely used in the research on the thermodynamic and dynamic characteristics of protein denaturation. We can verify whether high-pressure treatment affects the denaturation of PPI through DSC experiment. Table 7.8 shows the

Table 7.8 DSC scanning of PPI samples at different pressures

Sample	T_{d1} (°C)	T_{d2} (°C)	△T1/2 (°C)	△H (J/g)
Control	93.53 ± 0.27	107.25 ± 0.09	6.35 ± 0.12	8.780 ± 0.58
50 MPa	93.4 ± 0.27	106.84 ± 0.01	6.86 ± 0.52	7.2 ± 0.74
80 MPa	93.01 ± 0.65	107.09 ± 0.09	6.74 ± 0.20	6.99 ± 0.61
100 MPa	92.44 ± 0.31	105.74 ± 0.75	6.4 ± 0.07	6.44 ± 0.32
150 MPa	–	106.73 ± 0.22	6.33 ± 0.15	6.08 ± 0.5
200 MPa	–	107.09 ± 0.01	6.16 ± 0.02	6.05 ± 0.12

analysis results of the impact of different pressures on the thermal characteristics of PPI: T_d is the denaturation temperature; T_d value can reflect the thermal stability of the protein; the higher the T_d, the higher the thermal stability is; and the lower the T_d, the lower the thermal stability is (Wang et al. 2000). △H is the enthalpy of the sample; exactly, it is the enthalpy change of the sample, that is, the ΔH before and after the thermal transformation of the sample can reflect the degree of denaturation of the protein, and the reaction of destroying hydrogen bond can produce the endothermic enthalpy, the protein agglomeration and the hydrophobic reaction can produce heat release enthalpy, and the enthalpy size and positive and negative results indicate which reaction is dominant. Half-peak width (△T1/2) mainly reflects the synergism of proteins during thermal denaturation.

As shown in Table 7.8, endothermic peak of untreated PPI occurred at 93.53 °C and 107.25 °C. According to the literature, PPI was mainly composed of arachin and conarachin. The research of Du Yin (2012) showed that the denaturation temperatures of arachin and conarachin were 102.27 °C and 87.49°C, respectively. Thus, 93.53 °C and 107.25 °C were the endothermic peaks of conarachin and arachin in PPI, respectively. As can be seen from the table, with the increase in pressure (50–100 MPa), the peak temperature of conarachin gradually decreased; at 150 MPa and 200 MPa, the endothermic peak of PPI was not visible, indicating that after high-pressure treatment, significant denaturation occurred in conarachin (this is basically the same as the SDS-PAGE electrophoretic result in 2.2.5). It was shown from the table that after high-pressure treatment, the endothermic peak of arachin was visible, showing that after the treatment at different pressures, arachin was more stable than conarachin and the temperatures of endothermic peak value changed. At the pressure of 100 MPa, the peak temperature was the lowest, being 105.74 °C and decreasing by 1.51 °C compared with the control. These results indicated that high pressure had different effects on conarachin and arachin. After 150 MPa, the endothermic peak of conarachin disappeared completely, but the endothermic peak of arachin was visible, showing that conarachin was more likely to denature than arachin under the action of pressure.

The study of Arntfield and Murray (1981) showed that the total enthalpy (△H) of glycinin and β-conglycinin represented the impact on the proportion of undenatured proteins in the sample or the proteins with ordered structure after pressure treatment. The total enthalpy (△H) of PPI after pressure treatment was lower than that of PPI without pressure treatment. With the increase of pressure,

Table 7.9 DSC scanning of PPI sample after treatment for different times

Sample	Td1 (°C)	Td2 (°C)	△T1/2 (°C)	△H(J/g)
Control	93.53 ± 0.27	107.25 ± 0.09	6.35 ± 0.12	8.780 ± 0.58
3 min	91.88 ± 0.57	106.64 ± 0.1	6.87 ± 0.02	10.14 ± 0.42
5 min	92.44 ± 0.31	105.74 ± 0.75	6.4 ± 0.07	6.44 ± 0.32
7 min	91.90 ± 0.01	106.54 ± 0.15	6.65 ± 0.07	10.18 ± 0.48
10 min	91.55 ± 0.19	106.43 ± 0.08	6.91 ± 0.16	9.61 ± 012
15 min	92.15 ± 0.3	106.56 ± 0.16	6.82 ± 0.21	9.13 ± 0.04

enthalpy decreased gradually, showing that with the increase of pressure, the degree of denaturation of PPI increased gradually, PPI unfolded gradually under the action of pressure, and the three-dimensional structure gradually became disordered, so that PPI was in a gradually unstable state, resulting in the decrease of energy required. The half-peak width of peak value of arachin was related to the transformation and coordination between the natural state and denatured state of protein (Privalov 1982), and it was not affected when treatment is at 50–200 MPa, as shown in Table 7.8. This showed that pressure did not change the coordination of protein denaturation.

2. Time

The DSC scanning results of PPI not treated at high pressure and PPI after treatment for 3–15 min at 100 MPa are shown in Table 7.9. It was shown from the table that the endothermic peaks of arachin and conarachin of PPI were visible after treatment for different times, but peak value temperature decreased compared to that of untreated PPI, showing that PPI did not denature completely after treatment for 15 min at 100 MPa, which was entirely different from the impact of pressure on the thermal characteristics of PPI. It was also seen from the table that after the treatment for different times, the initial denaturation temperature and peak temperature decreased; the degrees of decrease were different due to different treatment pressures. It was shown from the table that the peak values of the conarachins in the samples decreased by 1.65, 1.09, 1.63, 1.98, and 1.38 °C, respectively, relative to untreated PPI, with a decrease range of not more than 2 °C; the peak values of arachins decreased by 0.64, 1.51, 0.71, 0.82, and 0.69 °C, respectively, relative to untreated PPI, with a decrease range of not more than 1 °C, except the value after treatment for 5 min. This showed that the impact on glycinin was large after treatment for 5 min, which could be seen from its enthalpy. It showed after comparing the peak value changes of conarachin and arachin in different samples that at a certain pressure, the impact of different treatment times on conarachin was greater than that of arachin. It was shown from the half-peak widths (△T1/2) of the samples that the impact of different treatment times on its half-peak width (△T1/2) was small, so we considered that time did not change the coordination of protein denaturation.

Table 7.10 DSC scanning of PPI samples with different concentrations

Sample	T_{d1} (°C)	T_{d2} (°C)	△T1/2 (°C)	△H (J/g)
Control	93.53 ± 0.27	107.25 ± 0.09	6.35 ± 0.12	8.780 ± 0.58
1%	92.52 ± 0.07	106.71 ± 0.08	6.62 ± 0.25	9.68 ± 0.2
5%	92.44 ± 0.31	105.74 ± 0.75	6.4 ± 0.07	6.44 ± 0.32
10%	91.23 ± 0.14	106.48 ± 0.25	7.0 ± 0.07	9.46 ± 0.21
15%	91.01 ± 0.1	106.64 ± 0.3	6.56 ± 0.03	9.47 ± 0.05
20%	91.84 ± 0.21	106.3 ± 0.23	5.81 ± 0.02	10.01 ± 0.05

3. Protein concentration

The DSC scanning results of PPI not treated at high pressure and PPI with a mass concentration of 1–20% after treatment at 100 MPa are shown in Table 7.10. It was shown from the table that in untreated PPI and PPI with a protein concentration of 1–20% after treatment at 100 MPa, the endothermic peaks of conarachin and arachin were visible, which was consistent with the impact of time on the thermal characteristics of PPI but entirely different from the impact of pressure on the thermal characteristics of PPI, indicating that the impacts of different ultrahigh treatment conditions on the thermal characteristics of PPI were different. This was mainly due to the change in the structure of PPI after ultrahigh-pressure treatment. The change law in its structure was discussed in Article 2.3 of this book. It was shown from the table that, after ultrahigh-pressure treatment, the peak values of the conarachins and arachins in the PPIs with different concentrations decreased, which showed that after ultrahigh-pressure treatment, PPI denatured and thus its thermal stability decreased. Generally, the formation of a unique three-dimensional protein structure was the net result of various repulsive and attractive non-covalent interactions and several disulfide bonds, while denaturation asked to destroy these interactions. The decrease in denaturation temperature and denaturation enthalpy showed that the energy that required these interactions also decreased and the structure of PPI after ultrahigh-pressure treatment was loose. The reason might be because part of the interactions was destroyed or disulfide bonds were exposed to the surface of the protein molecule and some of the disulfide bonds were broken and thus protein molecules partially denatured. From the half-peak widths (ΔT1/2) of different samples in the table, the protein concentration had a slight impact on changing the coordination of protein denaturation.

3 Changes in Advanced Structure

Because the functional characteristics of natural PPI cannot meet the needs of production and products, it is generally used after modification. After ultrahigh-pressure physical modification, the gel properties of PPI were improved and at the same time changed its water-binding capacity, oil-binding capacity, particle size,

and microscopic characteristics (the results are shown in Articles 2.1 and 2.2), and the reason of these changes was because protein structure changed due to ultrahigh-pressure treatment. PPI has the characteristics of typical globulin. Studies have shown that the primary structure of protein determines the nutritional characteristics of protein, the high-level structure determines the functional properties of protein, and there is no the report on the impact of ultrahigh-pressure treatment on the primary structure of protein, so it is generally considered that ultrahigh pressure does not have any impact on the primary structure of protein; among the high-level structures, the quaternary structure of protein is the most difficult to obtain. Because the subunits of PPI are complex and it is difficult to separate and purify PPI to obtain individual subunits, there is no report on the study of the quaternary structure of PPI after ultrahigh-pressure treatment. In contrast to the primary and quaternary structures of protein, the study on secondary and tertiary structures of proteins is easier from the means of research or obtaining the detected samples. At present, there are some preliminary reports on the α-helix, β-sheet, and β-turn conformation and surface hydrophobicity in the protein after ultrahigh-pressure treatment, but the correspondence between the structural change and the functional change is not clear. Therefore, the research team has studied the relationship between the change laws of gel characteristics as well as secondary and tertiary structures during the process of ultrahigh-pressure treatment, so as to find out the inherent causes of the change of protein gel characteristics.

3.1 Secondary Structure

According to the energy size at the level after electron transition, the CD spectrum of protein was divided into three wavelength ranges: far-UV spectral region of below 250 nm, the circular dichroism of which was mainly caused by $n \rightarrow \pi^*$ electron transition of peptide bond; near-UV spectral region of 250–300 nm, the circular dichroism of which was mainly caused by $\pi \rightarrow \pi^*$ electron transition of peptide bond of side chain aromatic group; and UV-visible light spectrogram of 300–700 nm, the circular dichroism of which was mainly caused by external chromophore such as the prothetic group of protein (Sreerama and Woody 2004; Hanchang et al. 2007). Far UV CDs could be used to characterize the impact of ultrahigh pressure on the secondary structure of PPI, and the far-UV CD spectra of different samples after ultrahigh-pressure treatment (including different pressures, different times, and different concentrations) are shown in Figs. 7.21, 7.22, and 7.23. Tables 7.11, 7.12, and 7.13 showed the changes of the secondary structures of untreated PPI and PPI after high-pressure treatment obtained through computer Reed's simulation based on the measured CD spectral line. It was shown from Table 7.11 that the conformation of natural PPI contained 9.6% α-helix, 32.1% β-sheet, 10.6% turn, and 47.7% irregular coil, core conformation (α-helix + β-sheet) accounted for 41.7%, random structure (turn + irregular coil) accounted for 58.3%, and at the same time β-folding and irregular coil conformation

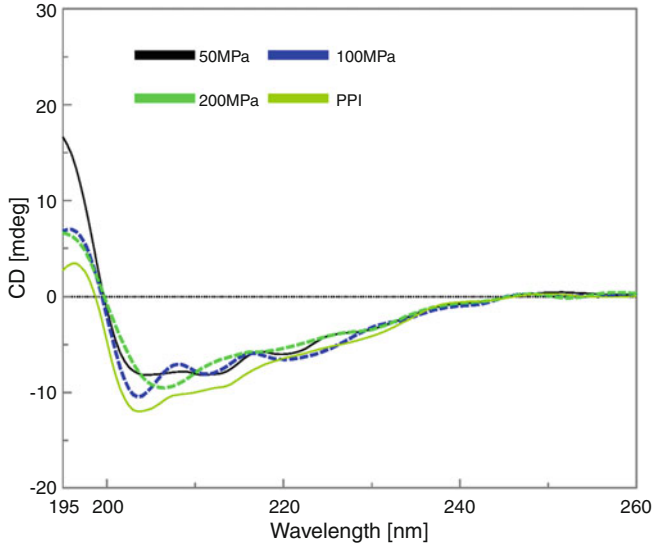

Fig. 7.21 CD spectrogram of PPI at different pressures

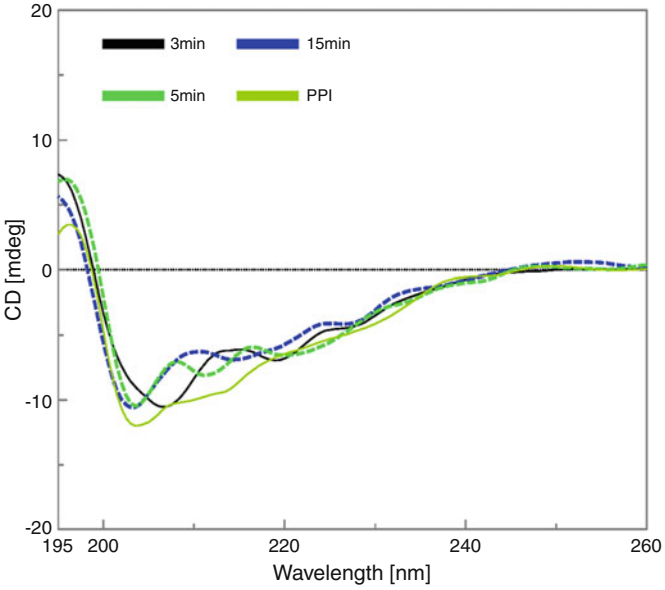

Fig. 7.22 CD spectrogram of PPI at different times

accounted for a large proportion. The CD spectra of protein were generally divided into two wavelength ranges, namely, 178–250 nm for the CD spectra of far-UV region and 250–320 nm for the CD spectra of near-UV region. The CD spectra of

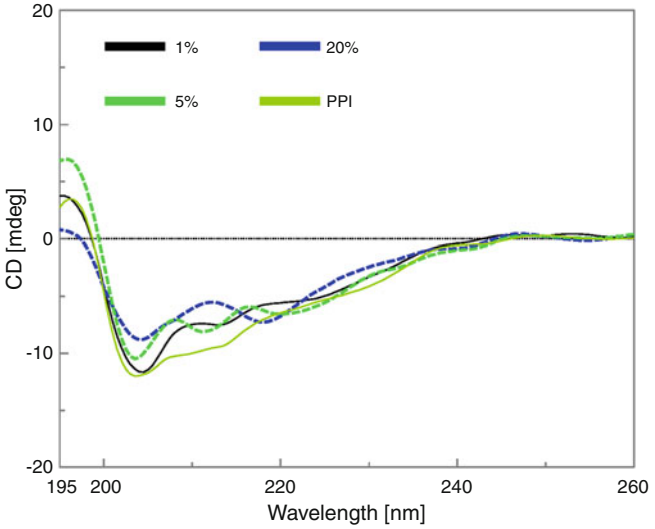

Fig. 7.23 CD spectrogram of PPIs with different concentrations

Table 7.11 Analysis of secondary structure of PPI at different pressures

	Reed's			
	α-Helix (%)	β-Sheet (%)	β-Turn (%)	Irregular coil (%)
PPI	9.6	32.1	10.6	47.7
50 MPa	35.0	0	29.5	35.5
100 MPa	41.4	3.2	15.5	39.9
200 MPa	25.2	15.0	17.9	41.9

Table 7.12 Analysis of secondary structure of PPI at different times

	Reed's			
	α-Helix (%)	β-Sheet (%)	β-Turn (%)	Irregular coil (%)
PPI	9.6	32.1	10.6	47.7
3 min	38.2	0	19.3	42.5
5 min	41.4	3.2	15.5	39.9
15 min	30.2	7.9	14.5	47.4

Table 7.13 Analysis of secondary structure of PPIs with different concentrations

	Reed's			
	α-Helix (%)	β-Sheet (%)	β-Turn (%)	Irregular coil (%)
PPI	9.6	32.1	10.6	47.7
1%	24.7	13.2	14.7	47.5
5%	41.4	3.2	15.5	39.9
20%	5.2	41.9	4.2	48.7

far-UV region reflected the circular dichroism of peptide bonds. In the regular secondary structures of protein or polypeptide, peptide bonds were arranged orderly, and the direction of arrangement decided the division of energy level transition of peptide bond. Therefore, the positions and absorption intensities of CD bands generated by proteins or polypeptides with different secondary structures were different. There was a positive band near 192 nm in α-helix structure, and there were two negative characteristic shoulder peak bands at 222 and 208 nm; there was one negative band at 216 nm in the CD spectrum of β-sheet, and there was one positive band at 185–200 nm; there was one positive CD band at 206 nm in β-turn, and there was negative CD band at the corresponding position of the left helix P2 structure. Therefore, the information on the secondary structures of protein or polypeptide chain could be reflected according to the far-UV CD spectrum of protein or polypeptide measured.

It was shown from Table 7.11 that the secondary conformation of PPI changed significantly after the treatment at different pressures. After the treatment at the pressures of 50, 100, and 200 MPa, PPI changed from mainly β-sheet and irregular coil conformation to α-helix conformation and β-turn conformation. Among them, α-helix conformation and β-turn confirmation significantly increased compared with untreated PPI, and α-helix conformations increased by 25.4%, 31.8%, and 15.6%, respectively, and β-turn confirmations increased by 18.9%, 4.9%, and 7.3%, respectively, while β-sheet conformation and irregular coil significantly decreased. At 50 MPa, there was no β-sheet conformation in PPI. With the increase of pressure, α-helix conformation in PPI first increased and then decreased, and β-sheet conformation first decreased to 0 and then increased with the increase of pressure. The contents of irregular coils decreased to different degrees and reached the minimum value under low-pressure treatment and then increased with the increasing pressure. It showed that α-helix played a major role and the hydrogen bond effect between proteins decreased during the pressure treatment. Turn conformation increased compared with natural PPI. With the increase of pressure, its content first increased and then decreased and reached the minimum value at 100 MPa. Most of β-turns were at the surface of protein molecule, and they could change the direction of polypeptide chain and made it bent, folded back, and reoriented. The change in the content of β-turn structure showed that the shape of PPI molecule might change, protein molecules extended, and the degree of asymmetry increased. It was shown from the table that at 50 MPa, the core conformation was 35%, not containing β-sheet conformation, and the random conformation accounted for 65%; at 100 MPa, the core conformation accounted for 44.6%, and the random conformation accounted for 55.4%; at 200 MPa, the core conformation accounted for 40.2%, and the random conformation accounted for 59.8%. This showed that under low pressure, there was almost no weak hydrogen-bonding interaction generated due to the dipole conversion in PPI. With the increase of pressure, the orderly structure in PPI first increased and then decreased, showing that during the pressure treatment, the protein first unfolded and then recombined due to the instable conformation of unfolded PPI.

The changes in the secondary conformations of PPI samples after different treatment times were shown in Table 7.12. It was shown from the table that at 3 min, the core conformations in the secondary conformations of PPI accounted for 38.2%, without β-sheet conformation, and the random conformations accounted for 61.8%; at 5 min, the core conformations accounted for 44.6%, and the random conformations accounted for 55.4%; at 15 min, the core conformations accounted for 38.1%, and the random conformations accounted for 61.9%. The change mechanism was similar to that of pressure sample.

From Table 7.13, it was shown that the changes in the secondary conformation of PPIs with different concentrations were significantly different. At low concentration (1%), the irregular coil conformations of PPI basically remained unchanged after treatment at100 MPa. They accounted for 47.7% and 47.5% before and after treatment, respectively, and there were changes only among α-helix, β-sheet, and β-turn conformations. When the concentration increased to 5%, the irregular coil decreased by 7.8% compared to that of untreated PPI; when the concentration increased to 20% again, the irregular coil slightly increased by 1% compared to that of untreated PPI. It was shown from the table that when the concentration was 1%, the core conformations accounted for 37.8% and the random conformations accounted for 62.2% in the secondary conformations of PPI; when the concentration was 5%, the core conformations accounted for 44.6%, and the random conformations accounted for 55.4%; when the concentration was 20%, the core conformations accounted for 47.1%, and the random conformations accounted for 52.9%. For the samples with a concentration of 20%, β-sheet and irregular coil conformations accounted for a large proportion in the secondary conformations of the samples after treatment at 100 MPa, and the untreated samples accounted for 90.6% and 79.8% in all the secondary conformations, respectively; α-helix and β-turn conformations accounted for a large proportion in the secondary conformations of the samples with a concentration of 1% or 5% after treatment at 100 MPa, accounted for 72.2% and 81.3% in all the secondary conformations, respectively. The above results showed that with the increase of concentration, the secondary conformations of PPI gradually became orderly and the protein structure extended.

In general, the ultrahigh-pressure treatment completely changed the secondary conformations of PPI, and the changes in the secondary conformations of PPI were completely different under different treatment conditions (including pressure, time, and concentration). Studies showed that high pressure had an impact on the change of the secondary conformation of PPI (Tu Zongcai 2007; Zhang 2001), and thus changes were caused by solubility, emulsification, and other functional characteristics. In this study, ultrahigh-pressure treatment not only changed the secondary conformations of PPI but also caused changes to gelation (see Figs. 7.1, 7.2, and 7.3). The following conclusions can be reached combining the results of the two: appropriate ultrahigh-pressure treatment can increase the relative contents of α-helix and irregular coil conformations in the secondary conformations of PPI, and such changes are advantageous to the formation of PPI.

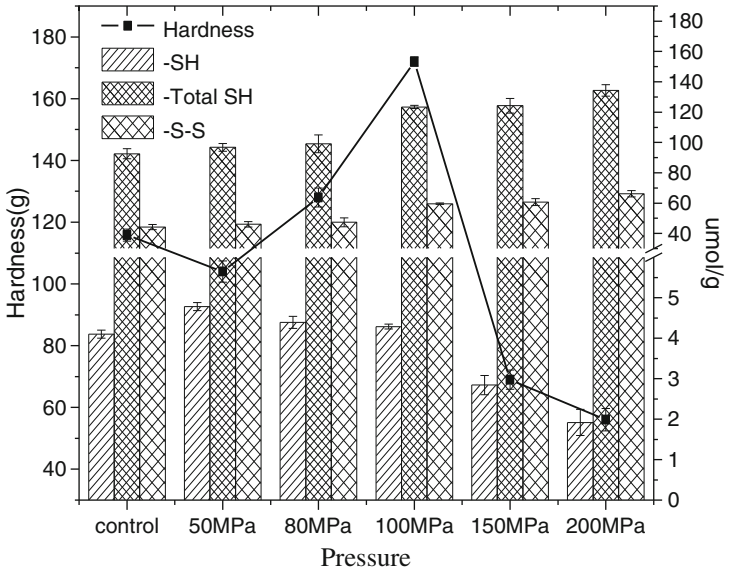

Fig. 7.24 Analysis of sulfhydryl and disulfide bond content in PPI at different pressures

3.2 Sulfhydryl and Disulfide Bonds

Sulfhydryl and disulfide bonds are important functional groups of protein, so they play an important role in the functional characteristics of protein. The PPI without ultrahigh treatment and the impacts of different ultrahigh-pressure treatment conditions (different pressure, time, protein concentration) on the contents of sulfhydryl and disulfide bonds and the hardness of curdlan formed were shown in Figs. 7.24, 7.25, and 7.26. The sulfhydryl of protein (including free sulfhydryl and the sulfhydryl hidden in the hydrophobic groups of protein) and total sulfhydryl group (including sulfhydryl and reduced disulfide bonds) were shown in the figure (Wu 2010). It was shown from Fig. 7.24 that the content of sulfhydryl in the PPI not treated at ultrahigh pressure was 4.10 μmol/g pro, which was close to the sulfhydryl content in ovalbumin (4.0 μmol/g pro); higher than skimmed milk (μmol/g pro), flour (2.18 μmol/g pro), and β-lactoglobulin (0.95 μmol/g pro) (Luo Mingjiang et al. 1986); and lower than egg white (50.7 μmol/g pro) (Luo Mingjiang et al. 1986), peanut-concentrated protein (9.09 μmol/g pro) (free sulfhydryl) (Wu 2009), and PPI (12.1 μmol/g pro) (free sulfhydryl). The total sulfhydryl content was 92.53 μmol/g pro, and the disulfide bond content was 44.22 μmol/g pro, which were higher than peanut-concentrated protein (26.22 μmol/g pro) and soy protein (23 μmol/g pro) (Wu 2009) and lower than egg white (79.7 μmol/g pro). Compared with the untreated PPI, with the increase of pressure, the total sulfhydryl content of PPI gradually increased, and sulfhydryl content first increased and then decreased. The sulfhydryl contents in the PPIs after treatment at 150 MPa and 200 MPa decreased

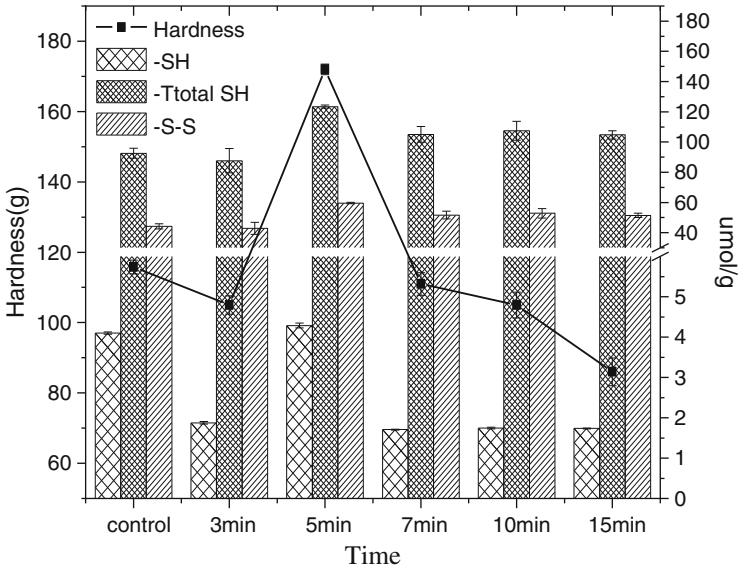

Fig. 7.25 Analysis of sulfhydryl and disulfide bond content in PPI at different times

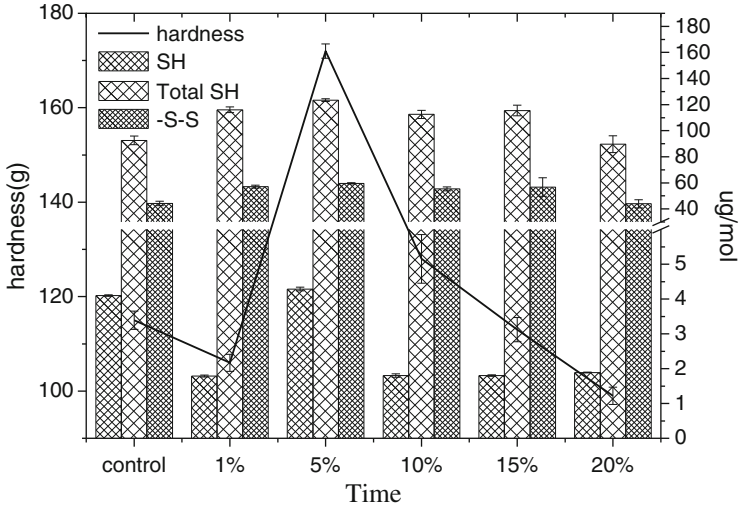

Fig. 7.26 Analysis of sulfhydryl and disulfide bond contents in PPIs with different concentrations

to 2.84 μmol/g pro and 1.92 μmol/g pro, which were all lower than that of untreated samples. This indicated that the pressure caused a significant change in the conformation of PPI, unfolding occurred in PPI, and the sulfhydryls at cysteine residues originally hidden in protein molecules were gradually exposed. However, after the pressure exceeded 100 MPa, the sulfhydryl content in PPI gradually decreased,

which might be caused due to -S-S bond combined by exposed sulfhydryls and other groups; therefore, with the increase of pressure, the content of disulfide bond in PPI gradually increased (Wu 2010; Yin Shouwei and Tang Chuanhe 2009). It was shown from the above results that although the pressure contributed to the exposure of the sulfhydryl in PPI, the sulfhydryl exposed in PPI reacted with other groups due to instable structure of PPI treated at a certain pressure. It was also shown from Fig. 7.24 that when the total sulfhydryl content in PPI was 123.39 μmol/g pro, the sulfhydryl content was 4.29 μmol/g pro, and the disulfide bond content was 59.55 μmol/g pro; the PPI gel hardness reached the maximum value.

The above results showed that the three-dimensional structure of peanut changed locally due to ultrahigh-pressure treatment technology. Under the action of ultrahigh pressure, protein molecules might meet the following two cases. First, the protein molecules become loose, the internal disulfide bonds were exposed to the molecular surface, some molecules had more violent activities locally, disulfide bond was broken and reduced to form sulfhydryl, and sulfhydryl content increased. Second, the sulfhydryl groups in protein molecules were also exposed to the molecular surface, and part of them fully combined with the oxygen in the air to form disulfide bonds; in addition, the sulfhydryl groups at the surface of protein molecules were surrounded in the molecules during the protein oxidation and refolding process, so sulfhydryl content decreased. In these two cases, when the pressure was smaller than 100 MPa, the first case was dominant, so that the sulfhydryl content of peanut increased with the increase of pressure; when the pressure was greater than 100 MPa, with the increase of treatment pressure, the second case became the main process of structural change, and thus sulfhydryl content showed a decreasing trend. In general, the sulfhydryl content of PPI after ultrahigh-pressure treatment increased compared with the untreated original sample.

The changes in the sulfhydryl and disulfide bond contents of untreated PPI and PPI that have been treated at 100 MPa for 3–15 min and the hardness after forming curdlan were shown in Fig. 7.25. It was shown from the figure that compared with untreated PPI, the sulfhydryl and total disulfide bond contents of PPI after ultrahigh-pressure treatment first decreased and then increased sharply and the contents of the two reached the maximum values at 5 min, they decreased sharply at 7 min, and the changes in the two slowed down after extending the time. Disulfide bond content first increased and then decreased gradually with the continuous extension of time, and it reached the maximum value at 5 min, which was basically consistent with the change in the hardness of sample after forming curdlan; the hardness of sample reached the maximum value at 5 min. The results showed that the conformation of PPI had completely changed, the protein was de-folded, and more amino acid residues increased. Due to this, the total sulfhydryl content and sulfhydryl in the sample increased sharply after ultrahigh-pressure treatment for 5 min, the active sulfhydryl content decreased significantly, and total sulfhydryl content also decreased after continuing to extend the pressure application time. Its gel hardness was positively correlated with the influence of sulfhydryl content, the hardness reached the maximum value after high-pressure

treatment for 5 min, and later the hardness obviously decreased with the extension of time.

The changes in the sulfhydryl and disulfide bond contents of untreated PPI and PPI with a mass concentration of 1–20% after treatment at 100 MPa and the hardness after forming curdlan are shown in Fig. 7.25. It was shown from Fig. 7.26 that under the treatment conditions at 100 MPa, the total sulfhydryl and total disulfide bond contents of PPIs with different mass concentrations first increased and then decreased and the contents of the two in the sample reached the maximum values at the protein concentration of 5%, being 123.39 μmol/g pro and 59.55 μmol/g pro, respectively; the change trend was basically the same as that of hardness after forming curdlan. Compared with the untreated samples, the sulfhydryl content first decreased and then increased sharply with the increase of protein concentration; the sulfhydryl content reached the maximum value when the concentration was 5%, being 4.29 μmol/g pro, it decreased sharply at 7 min, and the sulfhydryl content changed slowly after continuing to increase the concentration, and this change trend was the same as that of the impact of different times on sulfhydryl content of PPI.

Studies showed that some processing methods (such as heating and high pressure) might result in the breakage of sulfhydryl and disulfide bonds and thus caused protein denaturation. Disulfide bond and sulfhydryl were weak secondary bonds to maintain the tertiary structure of protein, and the changes in their contents could reflect the degree of protein denaturation. It was shown from the above results that the contents of disulfide bond and sulfhydryl changed significantly during the ultrahigh-pressure treatment, which had an adverse impact on its functional characteristics such as gelation. In general, the heat gelation separation of PPI could be improved after treatment for 5 min at appropriate high pressure (such as 100 MPa).

3.3 Surface Hydrophobicity

ANS was used as fluorescence probe to measure the surface hydrophobicity indexes of PPI before and after ultrahigh-pressure treatment, and the results are shown in Fig. 7.27. Because the fluorescence spectrum of ANS was very sensitive to environmental changes, it was very sensitive to the conformational change of protein molecules. It was shown from the figure that with the increase of pressure, the surface hydrophobicity indexes of PPI first increased and then decreased, and they all increased obviously compared with that of control ($p < 0.01$). In the protein molecules not treated at ultrahigh pressure, most of the aromatic amino acid molecules that could produce fluorescent were in the protein and surrounded by a variety of nonpolar amino acid residues, so the polarity of the local microenvironment was weaker than that of external aqueous solution of protein molecules, and the surface hydrophobicity was low; in protein denatured after ultrahigh-pressure treatment, the side chain group of the aromatic amino acid molecule was gradually exposed to the aqueous solution, and the polarity of the environment was increased,

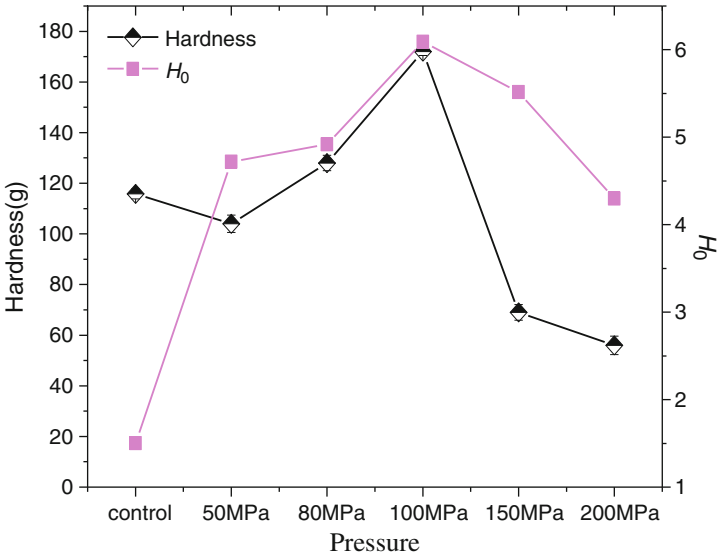

Fig. 7.27 Analysis of surface hydrophobicity indexes of PPI at different pressures

thus resulting in the increase of surface hydrophobic index. At the same time, it was shown from the figure that at 100 MPa, the surface hydrophobic index of PPI reached the maximum value, indicating that more hydrophobic groups in PPI were exposed to the outside and the protein structure was the most loose. After 100 MPa, the surface hydrophobic index of PPI gradually decreased, indicating that the structure of PPI was instable after pressure treatment and the folded protein might accumulate under the condition of increasing pressure. By comparing the changes in the surface hydrophobic index of PPI before and after ultrahigh-pressure treatment, it was shown that ultrahigh-pressure treatment might cause change to the conformations of PPI. And such change to the conformations might change the curdlan hardness of PPI. It was shown from the figure that, after treatment at different pressures, the change trends of surface hydrophobicity index and gel hardness of PPI were basically the same and they all reached the maximum values below 100 MPa. This also indicated that relatively loose protein conformation contributed to gel formation.

The change trends of surface hydrophobic index and gel hardness of untreated PPI and PPIs with different concentrations after treatment at 100 MPa for different times (5–15 min) were shown in Figs. 7.28 and 7.29. It was shown from Figs. 7.28 and 7.29 that the surface hydrophobic index and gel hardness of the samples significantly changed, but the change trends were basically consistent with each other, indicating that at 100 MPa, time and concentration had similar impacts on the exposure of hydrophobic groups in PPI. It was also shown from Figs. 7.28 and 7.29 that when the time was less than 5 min and protein concentration was less than 5%, the amino acid side chain group extended more fully with the extension of time;

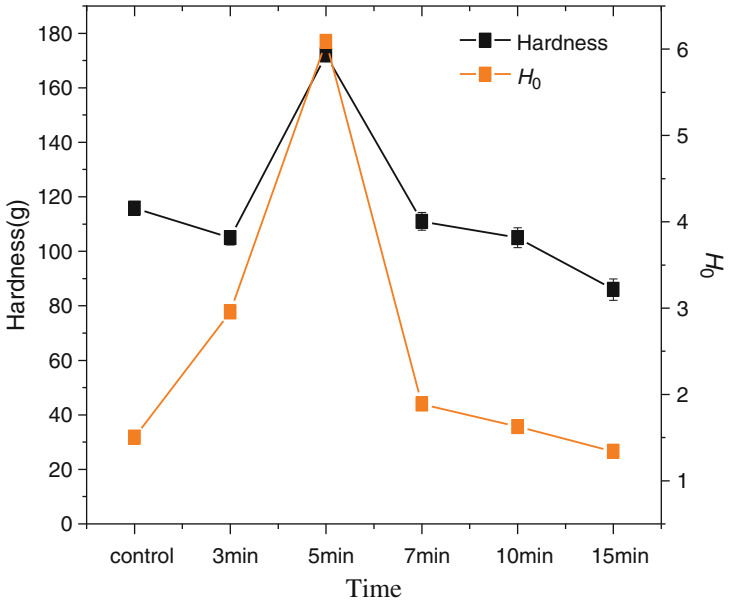

Fig. 7.28 Analysis of surface hydrophobicity indexes of PPI at different times

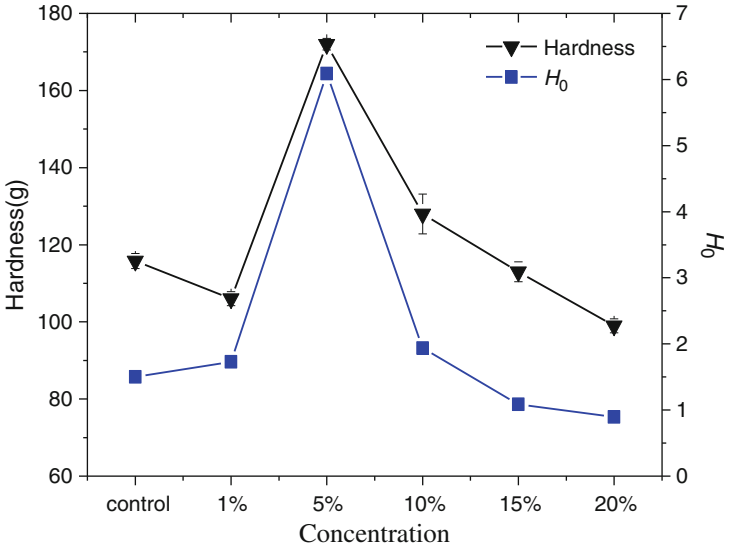

Fig. 7.29 Analysis of surface hydrophobicity of PPIs with different concentrations

more side chains of aromatic amino acid molecules among the protein molecules were exposed, and the hydrophobicity of the samples increased and reached the maximum values at 5 min and 5%, respectively; when the time was greater than

5 min, the expanded proteins reaggregated; when the concentration was greater than 5%, the gaps in aqueous solution became smaller due to the increase of concentration, and protein also reaggregated, resulting in a significant decrease in hydrophobic index.

ANS fluorescence probe method is a classic method to evaluate the surface hydrophobicity of protein, which is a reaction of protein three-dimensional structure in aqueous solution. We can analyze the changes in the three-dimensional structure of protein by observing the changes in the surface hydrophobicity of protein (Molina et al. 2001). Studies showed that hydrophobicity was the primary force to fold proteins into unique three-dimensional structures, and it had a significant impact on the functional characteristics of protein, such as solubility, emulsification, and foamability (Li Ying-qiu and Chen Zheng-xing 2006). After high-pressure treatment, the hydrophobicity of PPI first increased and then decreased, the change trend of which was basically the same as the curdlan formed, indicating that hydrophobicity had a significant impact not only on the solubility, emulsification, foamability, and other functional characteristics of protein but also on its gelation. Proper pressure and treatment time could improve the surface hydrophobicity of protein and improve its gelation.

3.4 Internal Fluorescence Characteristics

The side chain groups of the aromatic amino acid residues in the protein had the characteristic to absorb the incident light from the UV region and emit fluorescence, which could be used to study the changes in the overall spatial conformation of PPI during the ultrahigh-pressure treatment. When the excitation wavelength was 280 nm, the fluorescence spectrum which took tyrosine as the emission group was obtained. The impacts of different pressures, times, and concentrations on the fluorescence spectrum of tyrosine in PPI are shown in Figs. 7.30, 7.31, and 7.32. It was shown from the figures that the maximum fluorescence spectrum of tyrosine moved to the direction of long wave under the conditions of pressure, time, and concentration. With the increase of pressure and PPI concentration, the maximum fluorescence spectrum of tyrosine in PPI increased gradually, showing that the conformation change degree of PPI gradually increased under the treatment conditions of pressure and concentration; when the pressure was 200 MPa, the maximum fluorescence spectrum of tyrosine red shifted to 332 nm from 326.5 nm by 5.5 nm; when the concentration was 20%, the maximum fluorescence spectrum of tyrosine red shifted to 331.5 nm from 326.5 to 5 nm. It was shown that at different pressures and concentrations, the red shift degrees of maximum fluorescence spectrum of tyrosine in PPI were close to each other. This indicated that under these two conditions, the overall spatial conformation change degrees were close and the maximum fluorescence spectrum of tyrosine in protein red shifted, showing that the side chain groups of tyrosine molecules in protein were gradually exposed to aqueous solution, the polarity of the environment gradually increased, and thus

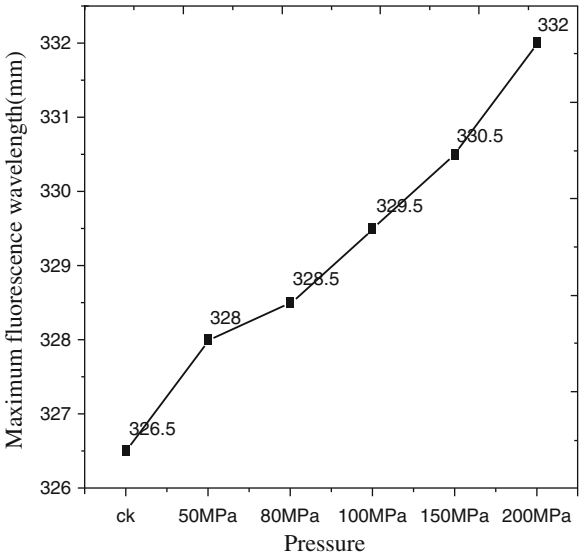

Fig. 7.30 Impact of pressure on the fluorescence wavelength of tyrosine in PPI

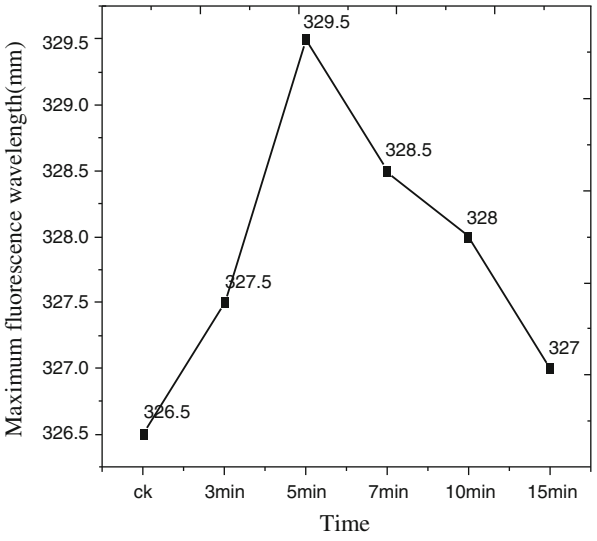

Fig. 7.31 Impact of time on the fluorescence wavelength of tyrosine in PPI

the maximum fluorescence wavelength moved to the direction of long wave. With the increase of time, the maximum fluorescence wavelength of tyrosine in PPI increased first and then decreased, indicating that in a short period of time, the space of PPI could be opened; however, after extending ultrahigh-pressure treatment time, the opened spatial conformation gradually became compact. However, it was shown from Fig. 7.31 that after treatment for 15 min, the maximum fluorescence wavelength of tyrosine in PPI red shifted (1 nm) compared with that of

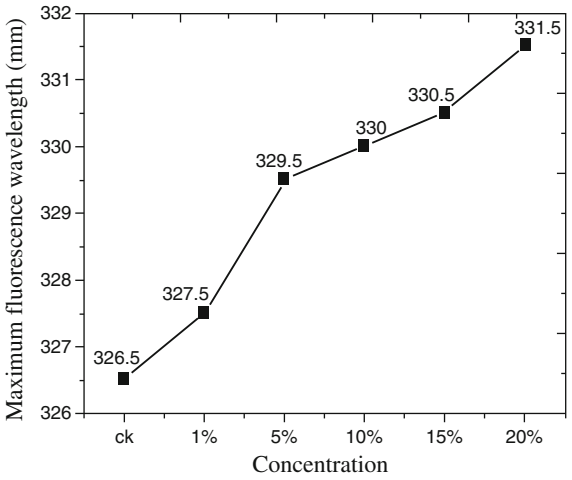

Fig. 7.32 Impact of concentration on the fluorescence wavelength of tyrosine in PPI

untreated PPI, indicating that the spatial conformation of PPI was not recovered to that before treatment.

The fluorescence spectrograms (Figs. 7.33, 7.34, and 7.35) showed the impacts of different pressures, times, and PPI concentrations on the fluorescence wavelength of PPI tryptophan when the excitation wavelength was 295 nm. Generally, the fluorescence of protein was provided by tryptophan residue, tyrosine residue, and phenylalanine residue. When the excitation wavelength was set to 295 nm, the fluorescence spectrum of protein was only provided by tryptophan residue. It was shown from the figure that with the increase of pressure and concentration and the extension of time, the maximum fluorescence wavelength of PPI tryptophan red shifted in different degrees compared with that of untreated PPI, showing that after ultrahigh-pressure treatment, the spatial conformation of PPI was destroyed, and thus the tryptophan residues in internal hydrophobic region were exposed to aqueous solution in different degrees, and PPI had more loose spatial structure than that before treatment. When the pressure was 200 MPa, the maximum fluorescence wavelength of PPI tryptophan red shifted from 329 to 335.5 nm by 6.5 nm; when the concentration was 20%, the maximum fluorescence wavelength PPI tryptophan red shifted from 329 to 336 Nm by 7 nm; under different pressure and concentration conditions, the red shift degrees of the maximum fluorescence wavelength of PPI tryptophan were close to each other, indicating that under these two conditions, the change degrees of overall spatial conformations were close to each other. When the treatment time was 7 min, the maximum fluorescence wavelength of PPI tryptophan red shifted from 329 to 333.5 nm by 4.5 nm; when the treatment time was 15 min, the maximum fluorescence wavelength of PPI tryptophan only red shifted by 1 nm compared with that before treatment, indicating that with the extension of time, the spatial structure of PPI gradually became compact from loose. The above results showed that the spatial conformation of PPI changed in a certain degree during the ultrahigh-pressure treatment.

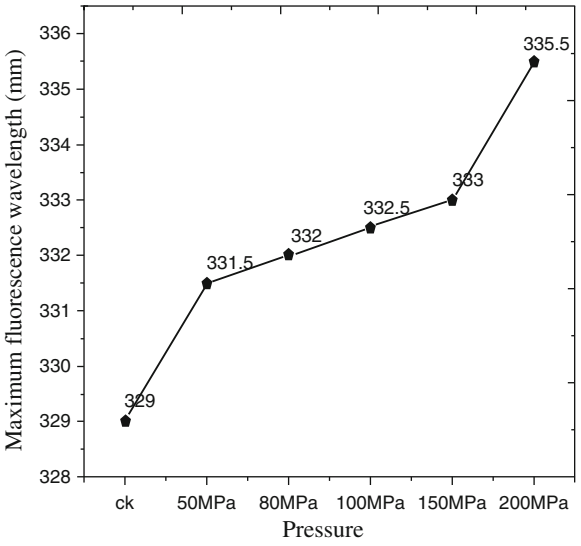

Fig. 7.33 Impact of pressure on the fluorescence wavelength of tyrosine in PPI

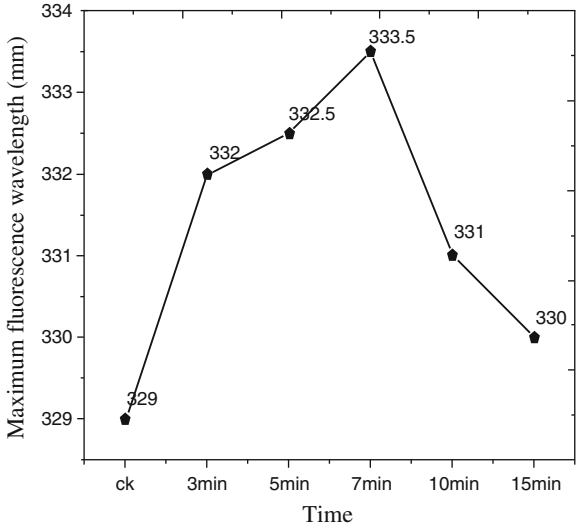

Fig. 7.34 Impact of time on the fluorescence wavelength of tyrosine in PPI

4 Correlation Among Gelation, Physicochemical Characteristics, and Structural Characteristics

Correlation analysis was conducted for the hardness, physicochemical characteristics of curdlan formed by 16 PPI samples, including those untreated and those after ultrahigh-pressure treatment (different pressures between 50 and 200 MPa, different times between 3 and 15 min, and different concentrations between 1% and

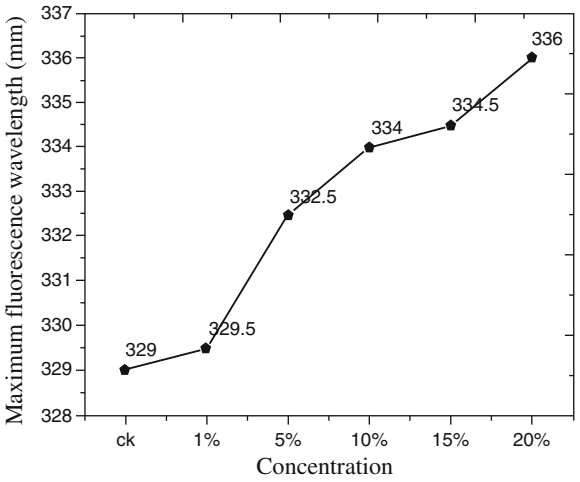

Fig. 7.35 Impact of concentration on the fluorescence wavelength of tyrosine in PPI

Table 7.14 Correlation among the indicators of PPI

Physicochemical characteristics		Structural characteristics	
	Gel hardness		Gel hardness
Oil-binding capacity	−0.035	SH	0.583*
Water-binding capacity	−0.320	Total SH	0.127
Particle size	−0.439	-S-S	0.075
Td1 (conarachin)	0.609**	H_0	0.432
Td2 (arachin)	−0.729**	Tyr fluorescence intensity	−0.237
△H	−0.213	Tyr fluorescence intensity	−0.132
$T_{1/2}$	0.052	α-Helix content	0.536
Cystine (%)	−0.390	β-Sheet content	−0.345
Hydrophobicity AA (%)	0.335	β-Turn content	−0.056
Polarity AA (%)	−0.311	Irregular coil content	−0.394

Note: df = 15, $\alpha_{0.05} = 0.482$, $\alpha_{0.01} = 0.606$, df = 9, $\alpha_{0.05} = 0.602$, $\alpha_{0.01} = 0.735$, *shows that 0.05 level is significant, **shows that 0.01 level is extremely significant

20%), as well as their tertiary structures. The sample sizes for the correlation analysis of secondary structure were 10, and the results were shown in Table 7.14. It was shown from the table that the correlation coefficient between gel hardness and the denaturation temperature of conarachin among physicochemical characteristics was 0.609, and they were positively correlated with each other significantly, and the correlation coefficient between it and the denaturation temperature of arachin was −0.727, and they were negatively correlated with each other significantly. This further showed that the denaturation of conarachin in PPI was aggravated, which was unfavorable to the increase of gel hardness, whereas arachin was opposite to it. At the same time, it was shown from the table that the

correlation coefficient of PPI gel hardness was −0.439, and they were negatively correlated with each other strongly. It was shown that the increase of PPI particle size was not conducive to the increase of gel hardness. Except the above physicochemical indicators, the correlation coefficient between PPI gel hardness and other physicochemical indicators was small with weak correlation.

It was shown from the correlation between PPI gel hardness and structural characteristics that the correlation coefficient between gel hardness and SH content in the sample was 0.583 and they were positively correlated with each other significantly, and the correlation coefficients between it and the surface hydrophobic index and α-helix content in the samples were 0.432 and 0.536, respectively, and they were positively correlated with each other strongly; in addition, the correlation coefficients between it and other structural characteristic indicators were small and the correlations were weak. This further indicated that the changes in SH content, surface hydrophobic index, and α-helix content would directly cause change to the gel hardness of sample, and the gel hardness of sample would increase with the increase of the contents of the above indicators in the sample. The analysis results of correlation between physicochemical characteristics and structural characteristics and gel hardness showed that although a series of changes occurred in the physicochemical characteristics and structural characteristics of PPI after ultrahigh-pressure treatment, there were only six indicators that had strong correlation with gel hardness, including the denaturation temperatures of conarachin and arachin in PPI, particle size, α-helix content, surface hydrophobicity index, and SH content. Among these six indicators, the indicators with the largest correlation were the denaturation temperatures of conarachin and arachin and SH content. This further showed that PPI gel hardness was improved mainly due to the action of the above factors.

Ultrahigh-pressure treatment significantly improved the thermal curdlan properties of PPI, the mechanism of which was mainly understood from the structural changes in the protein. It was found after analyzing the structure of PPI after ultrahigh-pressure treatment (including fluorescence spectra and circular dichroism spectrum) that the molecular structures of natural PPI were compact, the secondary structure was mainly composed of β-sheet (32.1%), the intramolecular hydrogen bond interaction was strong, and its contribution rate was 6.89%, and the secondary structure changed significantly after ultrahigh-pressure treatment, peptide bond was opened, and amino acid conformation changed to form the conformation mainly composed of α-helix. At 100 MPa, its content increased from 9.6% to 41.4%; while β-sheet decreased to 3.2%, the contribution rate of intramolecular hydrogen bond decreased to 3.42%; meanwhile, protein molecules unfolded; the microenvironment polarities of tyrosine and tryptophan increased; the maximum fluorescence wavelengths red shifted to 330.5 nm from 326.5 nm and 333 nm from 329 nm, respectively; a large number of hydrophobic groups were exposed; part of the hydrophobic groups between molecules formed a small amount of uniform aggregates through hydrophobic interaction reaction; and a large number of unreacted hydrophobic sites make the aggregates have very high surface hydrophobicity index. The surface hydrophobicity index of protein increased from 1.50 to 6.09, a

large amount of intramolecular free sulfhydryl were exposed, the total sulfhydryl content increased from 92.53 to 123.38 μmol/L, a small amount of disulfide bonds were broken, the adjacent free sulfhydryls form disulfide bonds through oxidation, and the content increased from 44.21 to 59.55 μmol/L. Due to the above structure changes, the PPI gel hardness was enhanced eventually.

References

Angsupanich K, Edde M, Ledward DA. Effects of high pressure on the myofibrillar proteins of cod and turkey muscle[J]. J Agric Food Chem. 1999;47(1):92–9.

Apichartsrangkoon A. Effects of high-pressure on rheological properties of soy protein gels [J]. Food Chem. 2003;80:55–60.

Arntfield SD, Murray ED. The influence of processing parameters on food protein functionality I. Differential scanning calorimetry as an indicator of protein denaturation. Can Inst Food Sci Technol J. 1981;14(4):289–94.

Arnfiled SD, Murray ED, Ismond MAH. Dependence of thermal properties as well as network microstructure and rheology on protein concentration for ovalbumin and vicilin [J]. J Texture Stud. 1990a;21:191–212.

Arnfiled SD, Murray ED, Ismond MAH. Influence of salts on the microstructural and rheological properties of heat-induced protein networks from ovalbumin and vicilin [J]. J Agric Food Chem. 1990b;38:1335–43.

Briscoe B, Luckham PF, Staeritz KU. Pressure induced changes in the gelation of milk protein concentrates [J]. Trends High Pressure Biosci Biotechnol, Proc. 2002;19:445–52.

Cong-Gui Chen, Borjigin Gerelt, Shao-Tong Jiang, Tadayuki Nishiumi, Atsushi Suzuki. Effects of high pressure on pH, water-binding capacity and textural properties of pork muscle gels containing various levels of sodium alginate. Asian Australas J Anim Sci. 2006;19 (11):1658–64.

Desrumaux A, Mareand J. Formation of sunflower oil emulsions stabilized by whey proteins with high-Pressure homogenization(up to 350 MPa): effect of pressure on emulsion characteristics [J]. Int J Food Sci Technol. 2002;37:263–9.

Du Yin. Study on the preparation and gel properties of the peanut protein fractions[D]. Beijing: Chinese Academy of Agricultural Sciences; 2012.

Gosal WS, Ross-Murphy SB. Gelation of whey protein induced by high pressure [J]. Curr Opin Colloid Interface Sci. 2005;34:188–94.

Hanchang H, Zhaofeng J, Zhu Hongji. The methods of protein conformation predicted by uv-circular dichroism [J]. Chemistry, 2007.

Hongkang Zhang, Lite Li, Eizo Tatsumi, Sabir Kotwal. Influence of high pressure on conformational changes of soybean glycinin. Innovative Food Sci Emerg Technol. 2003;4(3):269–75.

Jafari SM, He Y, Bhandari B. Production of sub-micron emulsions by ultrasound and microfluidization techniques [J]. J Food Eng. 2007;82:478–88.

Kolb G, Viardot K, Wagner G, et al. Evaluation of a new high-Pressure dispersion unit(HPN)for emulsification [J]. Chem Eng Technol. 2001;24:293–6.

Li Ying-qiu, Chen Zheng-xing. Effects of high pulsed electric field on hydrophobicity and sulfhydry groups content of soybean protein isolated [J]. Food Chem. 2006;27(05):40–2.

Luo Mingjiang, Luo Chunxia, Wu Ganxiang. Determination of sulfhydryl group and disulfuric chain of protein in food by Ellman's reagent colorimetric method [J]. J Zhengzhou Grain Coll. 1986;23:92–5.

Maruyama N, Katsube T, Wada Y, Moon Hun O, Rosa APBDL, Okuda E, Nakagawa S, Utsumi S. The roles of the N-linked glycans and extension regions of soybean beta-conglycinin in folding, assembly and structural features. Eur J Biochem. 1998;258(2):854–62.

Messens W, Van Camp J, Huyghebaert A. The use of highpressure modify the functionality of food proteins [J]. Trends Food Sci Technol. 1997;8:107–12.
Molina E, Papadopoulou A, Ledward DA. Emulsifying properties of high pressure treated soy protein isolate and 7S and 11S globulins. Food Hydrocoll. 2001;15(3):263–9.
Molina E, Defaye AB, Ledward DA. Soy protein pressure-induced gels. Food Hydrocoll. 2002;16 (6):625–32.
Murchie LW, Cruz-Romero M, Kerry JP, Linton M, Patterson MF, Smiddy M, Kelly AL. High pressure processing of shellfish: a review of microbiological and other quality aspects. Innovative Food Sci Emerg Technol. 2005;6(3):257–70.
Pinterits A, Arntfield SD. Improvement of canola protein gelation properties through enzymatic modification with transglutaminase. LWT Food Sci Technol. 2008;41(1):128–38.
Prakash V, Narasinga RMS. Physicochemical properties of oilseed proteins [J]. Crit Rev Biochem Mol Biol. 1986;20(3):286–98.
Privalov PL. Stability of proteins: proteins which do not presenta single cooperative system [J]. Adv Protein Chem. 1982;35:1–104.
Puppo C, Chapleau N, Speroni F, de Lamballerie-Anton M, Michel F, Añón C, Anton M. Physicochemical modifications of high-pressure-treated soybean protein isolates. J Agric Food Chem. 2004;52(6):1564–71.
Puppo MC, Speroni F, Chapleau N, de Lamballerie M, Añón MC, Anton M. Effect of high-pressure treatment on emulsifying properties of soybean proteins. Food Hydrocoll. 2005;19 (2):289–96.
Shi Yanguo, Sun Bingyu. The effects of ultrasonic wave on oil adsorption of alcohol precipitated soy protein concentrated [J]. Sci Technol Food Ind. 2005;26(10):84–86,89.
Sreerama N, Woody RW. Methods Enzymol [J]. 2004;383:318–51.
Tu Zongcai. Improvement of protein properties through dynamic high pressure micro-fluidization treatment and preliminary study on its mechanism [D]. Jiangxi: Nanchang University; 2007. p. 185–90.
Wang SM, Zhao JF, Huang MX, et al. Study on the mixed symergistic antioxidative activity from tea polyphenols and Vc to emulsion porkfat [J]. Sci Technol Food Ind. 2000;21(10):22–5.
Wang XS, Tang CH, Li BS, et al. Effects of high-pressure treatment on some physicochemical and functional properties of soy protein isolates[J]. Food Hydrocoll. 2008;22:560–7.
Wu HW. Study on preparation and gel-forming mechanism of peanut protein concentration and its application [D]. Beijing: Chinese Academy of Agricultural Science; 2009.
Wu W. Effects of protein oxidation on structure and gel properties of soy protein [D]. Wuxi: Jiangnan University; 2010. p. 25–6.
Xu ZR. Regression analysis and experimental design[M]. Beijing: China Agriculture Press; 1997. p. 102–58.
Yin Shouwei, Tang Chuanhe. Effect of micro-fluidization treatment on conformational and functional properties of kidney bean(Phaseolus vulgaris L.) protein isolates [J]. J South China Univ Technol. 2009;37(10):312–7.
Zhang HK. High pressure effects on biomacromolecules [D]. Beijing: China Agriculture University; 2001. p. 80–3.
Zhou SM. The function of the protein in the bakery product [J]. Cereal Oils. 1999;1:25–6.
Zong Wei, Chen Yi-ping. Effect of ultra high pressure on solubility of isolated peanut protein [J]. Cereals & Oils. 2007;10:16–7.
Zong Wei, Chen Yi-ping. Effect of ultra high pressure on the emulsifying ability of peanut protein isolate [J]. China Oils Fats. 2008;33(3):26–8.